ARTICLE

doi:10.1038/nature14658

Antibody against early driver of neurodegeneration *cis* P-tau blocks brain injury and tauopathy

Asami Kondo[1,2]*, Koorosh Shahpasand[1,2]*, Rebekah Mannix[3], Jianhua Qiu[3], Juliet Moncaster[4], Chun-Hau Chen[1,2], Yandan Yao[1,2], Yu-Min Lin[1,2], Jane A. Driver[1,5], Yan Sun[6], Shuo Wei[1,2], Man-Li Luo[1,2], Onder Albayram[1,2], Pengyu Huang[1,2], Alexander Rotenberg[6], Akihide Ryo[7], Lee E. Goldstein[4], Alvaro Pascual-Leone[8], Ann C. McKee[4], William Meehan[9], Xiao Zhen Zhou[1,2]§ & Kun Ping Lu[1,2]§

Traumatic brain injury (TBI), characterized by acute neurological dysfunction, is one of the best known environmental risk factors for chronic traumatic encephalopathy and Alzheimer's disease, the defining pathologic features of which include tauopathy made of phosphorylated tau protein (P-tau). However, tauopathy has not been detected in the early stages after TBI, and how TBI leads to tauopathy is unknown. Here we find robust *cis* P-tau pathology after TBI in humans and mice. After TBI in mice and stress *in vitro*, neurons acutely produce *cis* P-tau, which disrupts axonal microtubule networks and mitochondrial transport, spreads to other neurons, and leads to apoptosis. This process, which we term 'cistauosis', appears long before other tauopathy. Treating TBI mice with *cis* antibody blocks cistauosis, prevents tauopathy development and spread, and restores many TBI-related structural and functional sequelae. Thus, *cis* P-tau is a major early driver of disease after TBI and leads to tauopathy in chronic traumatic encephalopathy and Alzheimer's disease. The *cis* antibody may be further developed to detect and treat TBI, and prevent progressive neurodegeneration after injury.

Traumatic brain injury (TBI) is the leading cause of death and disability in children and young adults[1], and in the USA approximately 2.5 million people suffer TBI each year[2]. Nearly 20% of the 2.3 million troops deployed by the military have sustained TBI[3]. Repetitive mild TBI (rmTBI), seen in contact sports, or even single moderate/severe TBI (ssTBI), seen in military blasts, may cause acute and potentially long-lasting neurological dysfunction, including the development of chronic traumatic encephalopathy (CTE)[4–9]. TBI is also an established environmental risk factor for Alzheimer's disease[7–12]. However, no treatment is currently available to prevent CTE or Alzheimer's disease.

CTE is characterized by neurofibrillary tangles made of hyperphosphorylated tau[4–9]. Such tangles are also a hallmark of Alzheimer's disease and related neurodegenerative disorders, collectively termed tauopathies[13,14]. Tauopathy spreads in brains[15–19] and is reduced by immunotherapy against tauopathy epitopes[20–22]. However, since little tauopathy is detectable acutely or subacutely after TBI in humans and mice[5,7–9,23–25], whether tauopathy is a cause or consequence of post-traumatic neurodegeneration is unknown.

We have identified a unique proline isomerase, Pin1, that inhibits tauopathy in Alzheimer's disease by converting the phosphorylated Thr231-Pro motif in tau (P-tau) from *cis* to *trans* in Alzheimer's disease cell and mouse models[26–34]. In human Alzheimer's disease, Pin1 is inhibited by multiple mechanisms[27,29,35–37], whereas the Pin1 genetic polymorphism that prevents its downregulation is associated with delaying Alzheimer's disease age of onset[38]. In addition, Pin1 is located at a locus associated with late-onset Alzheimer's disease[39], P-tau appears early in pre-tangle Alzheimer's disease neurons[40], and its cerebrospinal fluid level correlates with memory loss in mild cognitive impairment and Alzheimer's disease[41]. We have developed antibodies that distinguish *cis* from *trans* P-tau and discovered that *trans* P-tau is physiological, promoting microtubule assembly, whereas the *cis* form is early pathogenic, leading to tauopathy in Alzheimer's disease[42]. Currently, it is unknown whether *cis* P-tau is present after TBI and if so, how to specifically eliminate it.

Robust *cis* P-tau in human CTE brains

We generated mouse monoclonal antibodies (mAbs) that, like our polyclonal antibodies[42], were able to distinguish *cis* from *trans* tau. We identified a *cis* mAb clone, 113, and a *trans* mAb clone, 25, with no cross-reactivity (Extended Data Fig. 1a, b). Both clones reacted to a pT231-tau peptide, but not its non-phosphorylated counterpart (Extended Data Fig. 1a, b).

We determined antibody binding affinities using a Biacore assay. *Cis* and *trans* mAbs specifically recognized the P-tau peptide (Fig. 1a, b), with their binding constants (K_D) being 0.27 and 42.1 nM, respectively (Table 1). Their IgG isotypes were IgG2b and IgG1, respectively (Extended Data Fig. 1c). Immunofluorescence and immunoblotting analyses showed robust *cis* signals in the soma and neurites, and *trans* signals in the soma in tau-transgenic mice, but not in tau-null

[1]Division of Translational Therapeutics, Department of Medicine, Beth Israel Deaconess Medical Center, Harvard Medical School, Boston, Massachusetts 02215, USA. [2]Cancer Research Institute, Beth Israel Deaconess Medical Center, Harvard Medical School, Boston, Massachusetts 02215, USA. [3]Division of Emergency Medicine, Children's Hospital Boston, Harvard Medical School, Boston, Massachusetts 02115, USA. [4]Alzheimer's Disease Center, CTE Program, Boston University School of Medicine, Boston, Massachusetts 02118, USA. [5]Geriatric Research Education and Clinical Center, VA Boston Healthcare System, Harvard Medical School, Boston, Massachusetts 02130, USA. [6]Department of Neurology, Children's Hospital Boston, Harvard Medical School, Boston, Massachusetts 02115, USA. [7]Department of Microbiology, Yokohama City University School of Medicine, Yokohama 236-0004, Japan. [8]Department of Neurology, Beth Israel Deaconess Medical Center, Harvard Medical School, Boston, Massachusetts 02215, USA. [9]Micheli Center for Sports Injury Prevention, Children's Hospital Boston, Harvard Medical School, Boston, Massachusetts 02115, USA.
*These authors contributed equally to this work.
§These authors jointly supervised this work.

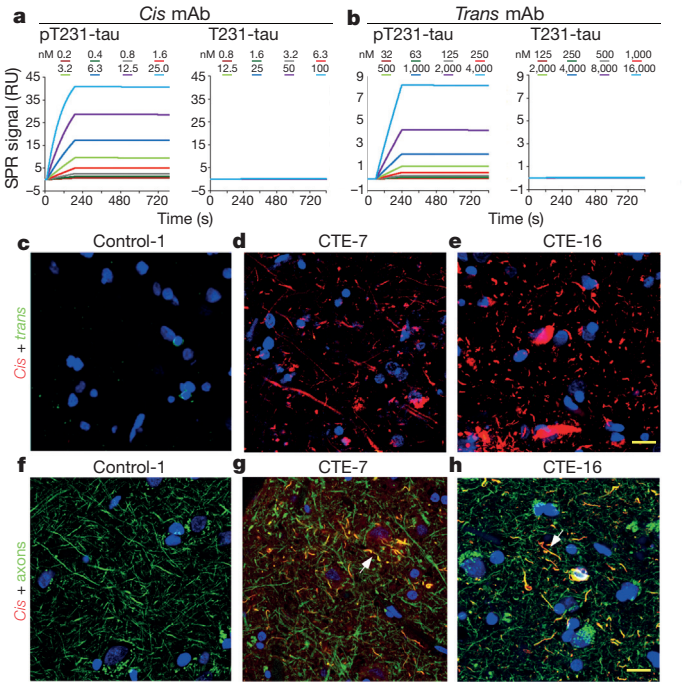

Figure 1 | Robust *cis*, but not *trans*, P-tau at diffuse axons in human CTE brains. **a**, **b**, *Cis* (**a**) or *trans* (**b**) mAb were immobilized on a sensor chip CM5 for surface plasmon resonance and their binding to pT231- or T231-tau peptide at different concentrations were recorded by SRP sensorgrams. **c**–**h**, The frontal cortex of neuropathologically verified human CTE brains and normal controls were subjected to double immunofluorescence with *cis* (red) or *trans* (green) mAbs (**c**–**e**), $n = 16$ for CTE and 8 for controls, or with *cis* pT231 (red) and the axonal marker tau (green), along with DNA dye (blue) (**f**–**h**), $n = 4$. Two typical *cis* P-tau immunostaining patterns are presented, with all cases being shown in Extended Data Fig. 1f, g. Arrows, colocalization; scale bars, 20 μm.

mice (Extended Data Fig. 1d, e). Thus, *cis* and *trans* mAb behave similarly to their polyclonal counterparts[42].

Since the T231-tau phospho-epitope is identical among species, we performed double immunofluorescence with *cis* and *trans* mAbs on CTE brain tissues from 16 patients with a history of TBI exposure and 8 healthy controls[6] (Supplementary Table 1). While *trans* mAb detected a few neurons in the soma in control and CTE brains, *cis* mAb detected no signal in control brains. However, robust *cis* mAb signals were observed in diffuse neurites in all CTE brains examined, with two typical patterns evident, distinguished by one with stronger *cis* P-tau signals, especially in soma (Fig. 1d, e and Extended Data Fig. 1f–h). *Cis* mAb co-localized with AT180 (recognizing pT231-tau), T22 (tau oligomers[43]), AT8 (early tangles), and AT100 and Alz50 (mature tangles), but *trans* mAb did not co-localize with T22 (Extended Data Fig. 2a, b). *Cis* P-tau was more concentrated near blood vessels (Extended Data Fig. 2c), as expected[6]. *Cis* P-tau co-localized diffusely with the axonal marker tau, but not the dendritic marker MAP2, in CTE brains (Fig. 1g, h and Extended Data Fig. 2d). Thus, *cis* P-tau localizes primarily to diffuse axons in CTE brains.

Cis P-tau is the earliest TBI tau epitope

To determine the temporospatial characteristics of *cis* P-tau induction after TBI, we used TBI mouse models induced by impact[25] and blast[5],

Table 1 | Binding affinities of *cis* and *trans* mAbs

mAb	Peptide	K_a (ms^{-1})	K_d (s^{-1})	K_D (nM)
Cis	pT231-tau	40,700	1.10×10^{-5}	0.27
Cis	T231-tau	0.17	1.00×10^{-5}	58,820
Trans	pT231-tau	250	1.05×10^{-5}	42.0
Trans	T231-tau	4.5	1.95×10^{-5}	4,333

The association rate constant (K_a), dissociation rate constant (K_d), and binding constant (K_D) of *cis* and *trans* mAbs towards pT231-tau or T231-tau peptide were determined by Biacore analysis.

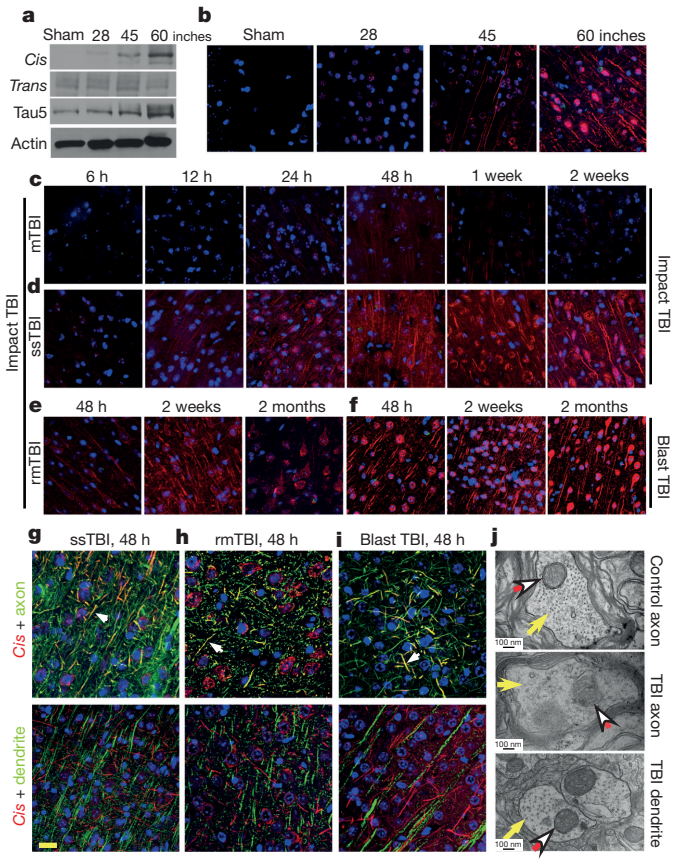

Figure 2 | While mTBI has moderate and transient effect, rmTBI, ssTBI or blast TBI leads to robust and persistent *cis* P-tau induction, notably in diffuse axons starting at 12–24 h. **a**, **b**, Mice were subjected to single TBI by a 54 g weight drop from varying heights, followed by immunoblotting (**a**) and immunofluorescence (**b**) to detect *cis* and *trans* P-tau 48 h later. *Cis*, red; *trans*, green; DNA, blue. **c**–**e**, Mice were subjected to single mTBI (**c**), ssTBI (**d**) or rmTBI (**e**), followed by immunofluorescence to detect *cis* and *trans* P-tau at different times after last injury. $n = 4$. **f**, Mice were subjected to blast-induced TBI, followed by immunofluorescence to detect *cis* and *trans* P-tau at different times. $n = 3$. **g**–**i**, ssTBI (**g**), rmTBI (**h**) and blast TBI (**i**) brain sections at 48 h after last injury were subjected to double immunofluorescence with *cis* pT231 (red) and axon marker neurofilament SMI312 (green) or dendrite marker MAP2 (green), along with DNA dye (blue). $n = 4$. Arrows, colocalization; magnification in **b**–**f**, ×63; scale bars in **g**–**i**, 20 μm. **j**, ssTBI or sham mice were subjected to electron microscopy analysis 48 h after injury to examine the structure of microtubules (filled arrows) and mitochondria (open arrows) at axons and dendrites. Scale bars, 100 nm.

modelling sport- and military-related TBI, respectively. 48 h after impact TBI, *cis*, but not *trans*, P-tau was elevated in a severity-dependent manner, correlating with total tau (Fig. 2a, b and Extended Data Fig. 3a, b), and reflecting the stability of *cis* P-tau[42]. While single mild TBI (mTBI) moderately and transiently induced *cis* P-tau, which returned to the baseline by 2 weeks, ssTBI robustly and persistently induced *cis* P-tau, starting at 12 h and peaking at 48 h, but sustaining high levels over time (Fig. 2c, d and Extended Data Fig. 3c). Both rmTBI and blast TBI also induced robust and persistent *cis* P-tau induction, with more profound effects in the latter (Fig. 2e, f and Extended Data Fig. 3c).

Robust *cis* P-tau signals were detected 48 h after TBI without tau oligomers, aggregation or tangle epitopes (Extended Data Fig. 3d, e, and see results later). *Cis* P-tau localized mainly to axons, but not dendrites in impact and blast TBI models (Fig. 2g–i), as in CTE brains (Fig. 1g, h and Extended Data Fig. 2d). *Cis* P-tau expression was associated with axonal injury with marked disruption of microtubules and mitochondria, which was notably absent in dendrites (Fig. 2j),

consistent with the fact that TBI mainly affects axons[44]. Thus, robust *cis* P-tau is induced acutely in axons after impact and blast TBI long before other forms of P-tau appear.

Cis P-tau spreads and is toxic after TBI

Further analysis showed *cis* P-tau spreading in the brain after TBI. *Cis* P-tau was mainly limited to the cortex from 24 h to 2 months after rmTBI, but 6 months after rmTBI, robust *cis* P-tau signals were detected in the cortex and other brain regions, including the hippocampus (Fig. 3a–c). Marked *cis* P-tau spread from the cortex to the hippocampus and even to the other side of the brain was observed after blast TBI (data not shown). To examine whether *cis* P-tau might be neurotoxic, brain lysates prepared from rmTBI and sham mice 6 months post-injury were added to growing cultured neurons overnight. *Cis*, but not *trans*, P-tau was readily detected in neurons treated with rmTBI lysates, but not when treated with sham controls (Fig. 3d). Compared with untreated or sham-treated controls, neurons treated with rmTBI lysates had much higher rates of apoptosis, which was rescued by immunodepletion of total tau or *cis*, but not *trans*, mAb (Fig. 3e). Thus, after impact and blast TBI, *cis* P-tau is robustly induced, spreads through the brain over time, and induces apoptosis that is blocked by *cis* mAb.

Stress induces *cis* P-tau, blocked by mAb

To understand how *cis* P-tau induces apoptosis and spreads through the brain, we examined the *in vitro* response to neuronal stress induced by serum starvation or hypoxia. Both conditions induced *cis*, but not *trans*, P-tau (Fig. 4a and Extended Data Fig. 4a, d), well before tau aggregation (Extended Data Fig. 4e). The addition of

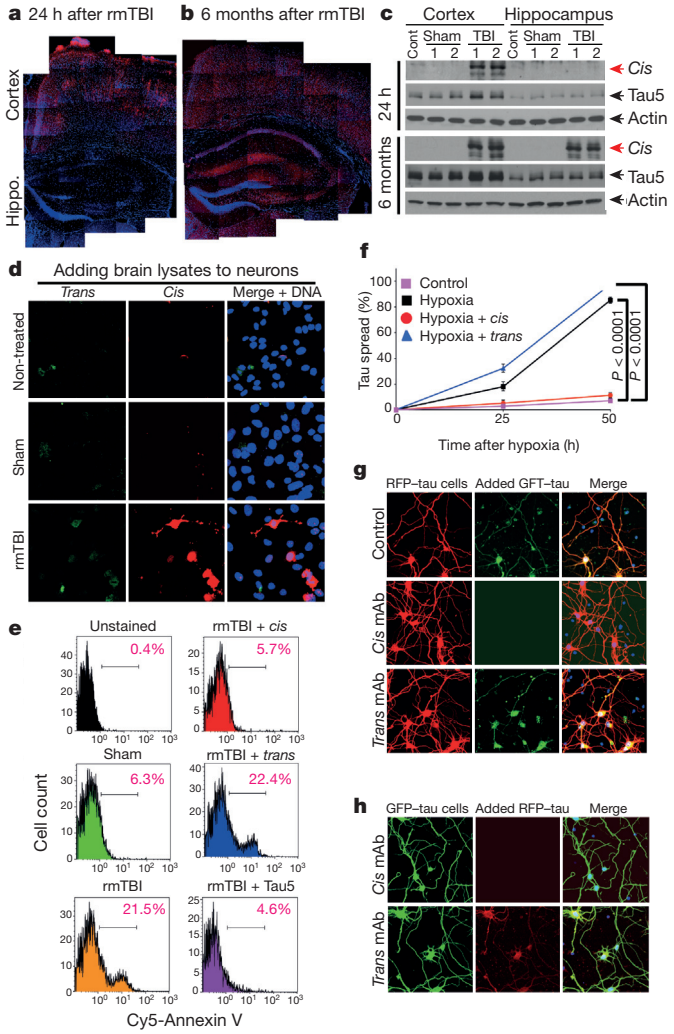

Figure 3 | *Cis* P-tau spreads in the brain after rmTBI, and spreads and causes neurotoxicity after neuronal stress *in vitro*, which are fully blocked by *cis*, but not *trans*, mAb. **a**–**c**, 24 h or 6 months after rmTBI, mouse brains were subjected to immunofluorescence (**a**, **b**) and immunoblotting (**c**) to detect *cis* P-tau in different brain regions. $n = 4$. **d**, **e**, Mouse brain lysates prepared from 6-month-post-rmTBI or sham controls were added to culture media of SY5Y neurons for 17 h directly or after immunodepletion with *cis* or *trans* mAb, followed by immunofluorescence with *cis* and *trans* mAbs or annexin V FACS. $n = 3$. **f**, SY5Y neurons stably expressing GFP–tau or RFP–tau were co-cultured and then treated with hypoxia or control in the presence or absence of *cis* or *trans* mAb for different times, followed by assaying cells expressing both GFP–tau and RFP–tau (mean ± s.d.). *P* values, two-way ANOVA test. **g**, **h**, Primary mouse neurons were transfected with GFP–tau or RFP–tau, and then subjected to hypoxia treatment in the absence or presence of *cis* or *trans* mAb for 36 h. The resulting filtered soluble media from GFP-expressing neurons was added to RFP-expressing neurons (**g**) or vice versa (**h**), followed by detecting entry of added tau.

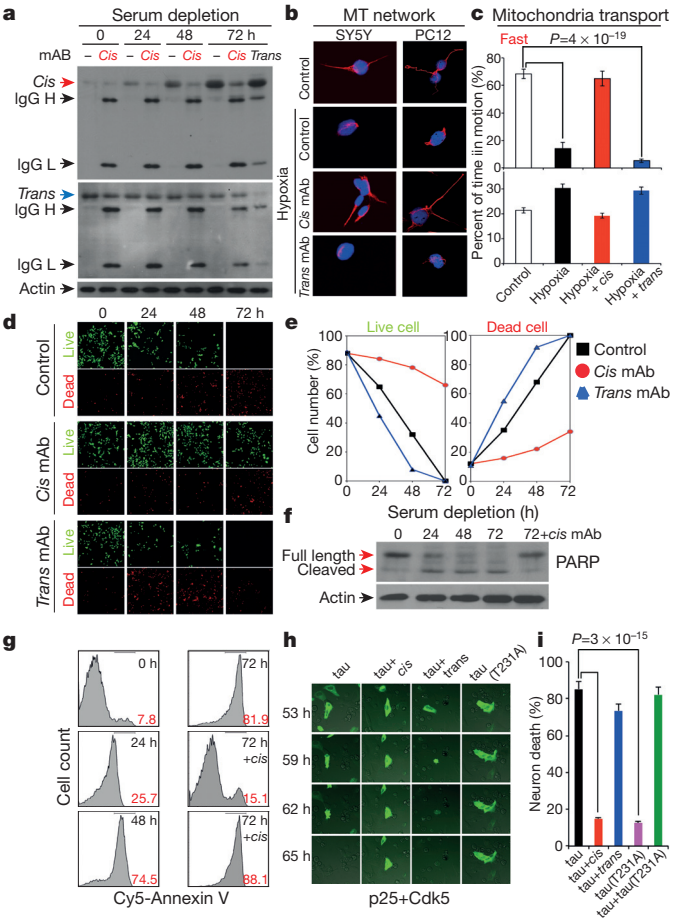

Figure 4 | Stressed neurons robustly produce *cis* P-tau leading to cistauosis, which is blocked by *cis* mAb, but enhanced by *trans* mAb. **a**, SY5Y cells were cultured without serum for different times in the absence and presence of *cis* or *trans* mAb, followed by immunoblotting for *cis* and *trans* P-tau. **b**, SY5Y and differentiated PC12 cells were treated with hypoxia in the absence and presence of *cis* or *trans* mAb for 48 h, followed by staining for microtubules. **c**, Differentiated PC12 cells were treated with hypoxia in the absence and presence of *cis* or *trans* mAb for 48 h, followed by live-cell microscopy to capture fast and slow transport of mitochondria along neurites. **d**–**g**, SY5Y cells were cultured without serum for different times in the absence and presence of *cis* or *trans* mAb, followed by live/dead cell assay (**d**, **e**) and apoptosis assays using PARP cleavage (**f**) and annexin V (**g**). **h**, **i**, SY5Y cells were co-transfected with GFP–tau or GFP–tau(T231A) and p25/Cdk5, followed by live-cell imaging to observe cell death of GFP–tau expressing cells over 65 h (**h**), with quantification being shown (**i**) (mean ± s.d.). *P* values, ANOVA test.

stressed neuron lysates to neurons induced cell death, which was rescued by immunodepletion with *cis*, but not *trans*, mAb, as detected by the live/dead assay (Extended Data Fig. 4g). To examine whether *cis* P-tau is implicated in tau spreading, we generated SY5Y cells stably expressing green or red fluorescent protein-conjugated tau (GFP–tau or RFP–tau), and co-cultured them with or without stress. Without hypoxia, neurons continued to express either GFP–tau or RFP–tau, but rarely both proteins (Fig. 3f and Extended Data Fig. 5b). However, consistent with *cis* P-tau spreading in TBI brains (Fig. 3a–c and Extended Data Fig. 5a), hypoxia induced *cis* P-tau (Extended Data Fig. 4d) and caused progressive tau spreading, which was prevented by *cis*, but not *trans*, mAb (Fig. 3f and Extended Data Fig. 5b). Moreover, serum-starved neurons released *cis*, but not *trans*, P-tau at 40 h before neuronal death at 72 h (Extended Data Fig. 4h). Similar patterns of *cis* P-tau spread and neurotoxicity were also observed in primary neurons and blocked by *cis*, but not *trans*, mAb (Fig. 3g, h, Extended Data Fig. 5c, d). Thus, toxic *cis* P-tau is induced and spreads after neuronal stress, similar to TBI.

Cis mAb blocks cistauosis after stress

Given the ability of *cis* mAb to block tau from spreading and inducing apoptosis, we examined whether *cis* or *trans* mAb could affect intracellular P-tau after stress. Indeed, *cis* mAb entered neurons and effectively blocked time-dependent *cis* P-tau induction, without affecting *trans* following serum starvation (Fig. 4a and Extended Data Fig. 4a) or hypoxia (Extended Data Fig. 4d). Conversely, *trans* mAb reduced *trans*, but not *cis*, P-tau (Fig. 4a), indicating that the two isomers are not readily interchangeable, as suggested in TBI (Fig. 2) or CTE (Fig. 1), and Alzheimer's disease[42].

Since Pin1 inhibition by downregulation[27,29], C113 oxidization[35] and S71 phosphorylation[36,37] contributes to tauopathy in Alzheimer's disease, we asked whether such Pin1 inhibition contributes to *cis* P-tau induction after stress. *Cis* induction correlated highly with Pin1 downregulation after serum starvation and Pin1 C113 oxidization after hypoxia (Extended Data Fig. 6a, b). Pin1 S71 phosphorylation was also markedly elevated in TBI brains (Extended Data Fig. 6c). Moreover, Pin1 knockdown enhanced *cis* P-tau induction by hypoxia, which was eliminated by *cis* mAb (Extended Data Fig. 6d). Since Pin1 knockout induces P-tau accumulation only in old mice[29,32,42] and stress activates Pro-directed kinases, increased tau phosphorylation may be also important for *cis* P-tau induction after stress or TBI.

Given the ability of *cis* mAb to ablate intracellular *cis* P-tau, we evaluated how *cis* mAb might enter neurons to remove *cis* P-tau. Tau mAbs enter neurons via Fcγ receptors[45] and mAbs trigger targeted protein degradation by the TRIM21-mediated proteasome pathway[46]. Indeed, blocking Fcγ receptors prevented *cis* mAb from binding to or entering neurons (Extended Data Fig. 7a–c). Immunogold electron microscopy showed *cis* mAb on the outer cell surface and in intracellular vesicles (Extended Data Fig. 7d). TRIM21 knockdown[46], but not the autophagy inhibitor 3-methyladenine (3-MA), prevented *cis* mAb from ablating *cis* P-tau (Extended Data Fig. 7e–g). Thus, *cis* mAb likely enters neurons via Fcγ receptors to target *cis* P-tau degradation.

To examine the functional significance of neuronal *cis* P-tau induction and elimination, we investigated whether *cis* P-tau might affect the microtubule network and function since *cis*, but not *trans*, P-tau loses its microtubule function[42]. Hypoxia not only induced *cis* P-tau (Extended Data Fig. 4d), but also caused microtubule collapse in neurites, an effect that was rescued by *cis*, but not *trans*, mAb (Fig. 4b and Extended Data Fig. 4b). Measuring mitochondria movement along neurites showed that hypoxia stopped microtubule-based fast transport, but not actin-based slow movement (Fig. 4c and Supplementary Videos 1, 2). This mitochondria transport defect was restored by *cis* mAb, but not *trans* mAb (Fig. 4c and Supplementary Video 3), with the latter even causing neurite retraction (Supplementary Video 4), probably by *trans*-associated promotion of microtubule assembly[42].

Serum starvation led to robust apoptosis by the time *cis* P-tau was highly induced, which was potently rescued by *cis*, but not *trans* mAb, as detected by a live/dead assay (Fig. 4d, e), PARP cleavage (Fig. 4f and Extended Data Fig. 4c) and annexin V fluorescence activated cell sorting (FACS; Fig. 4g). Similar results were obtained with hypoxia (Extended Data Fig. 4f), even in primary neurons (Extended Data Fig. 5c, d). Thus, neuronal stress robustly induces *cis* P-tau, which disrupts axonal microtubules and organelle transport, spreads to other neurons and leads to apoptosis. These phenotypes, potently rescued by *cis* but not *trans* mAb, are here termed 'cistauosis'.

To determine the importance of *cis* P-tau for neurotoxicity, we co-transfected neurons with GFP–tau or its T231A mutant and p25/Cdk5 phosphorylating tau on Thr231 and others[27,47]. Co-expression of tau, but not its T231A mutant, with p25/Cdk5 increased *cis* P-tau, which was eliminated by *cis* mAb (Extended Data Fig. 8a). Importantly, most GFP–tau-, but not GFP–tau(T231A)-expressing cells were dead by 62 h, which was markedly blocked by *cis* mAb, but accelerated by *trans* mAb (Fig. 4h, i and Supplementary Videos 5, 6). Thus, *cis* P-tau is necessary and sufficient for P-tau to induce neurotoxicity.

Cis mAb potently treats TBI and CTE

To evaluate the efficacy of *cis* mAb in treating TBI *in vivo*, we showed that *cis* or *trans* mAb were detected in brains 3 days after peripheral administration (Extended Data Fig. 9a). After treating ssTBI mice with *cis* mAb or IgG isotype control for 2 weeks, *cis* mAb effectively eliminated *cis* P-tau induction, both with and without pre-treatment (Fig. 5a and Extended Data Fig. 9b, d), and also potently reversed post-TBI ultrastructural pathologies of axonal microtubules and mitochondria (Fig. 5c and Extended Data Fig. 9f), defective cortical axonal long-term potentiation (LTP) (Fig. 5d and Extended Data Fig. 9g), and even apoptosis (Extended Data Fig. 9c), which is observed after TBI even in humans[48].

To determine the impact of *cis* mAb on behavioural or functional outcomes after TBI, we treated ssTBI mice with *cis* mAb for 2 months. There was no difference in hippocampal-dependent spatial memory between IgG and *cis* mAb-treated TBI mice (Extended Data Fig. 9h). However, as *cis* P-tau was concentrated in the medial prefrontal cortex at this time point (Fig. 3a), we used the elevated plus maze, an innate anxiety/risk-taking paradigm that involves cortical circuitry[49] and is affected by TBI[50]. All groups moved similar distances and times in the decision arm (Fig. 5e, f and Extended Data Fig. 10a–c). Sham mice stayed in the two closed or 'safe' arms (Fig. 5e, f and Extended Data Fig. 10a and Supplementary Video 7), but all IgG-treated ssTBI mice strikingly displayed 'risk-taking' behaviour, exploring the two open or 'aversive' arms (Fig. 5e, f and Extended Data Fig. 10a, b, and Supplementary Video 8), consistent with disinhibition likely due to a dysfunctional medial prefrontal cortex[49]. By contrast, *cis* mAb-treated mice exhibited minimal risk-taking behaviour, similar to sham mice (Fig. 5e, f and Extended Data Fig. 10a, and Supplementary Video 9).

To examine the effects of *cis* mAb on tauopathy development and spread, and brain atrophy, hallmarks of CTE[7–9], we treated ssTBI mice with *cis* mAb for 6 months. *Cis* mAb effectively prevented tauopathy development and spread, as assayed by *cis* P-tau, tau oligomers, aggregation and tangle epitopes (Fig. 5a, b, g, h and Extended Data Figs 9d, e and 10d, e), and brain atrophy in the cortex and white matter (Fig. 5i and Extended Data Fig. 10f). Thus, *cis* mAb not only eliminates *cis* P-tau and cistauosis, but also prevents tauopathy development and spread, restores LTP and behavioural defects, and prevents brain atrophy after TBI (Fig. 5j).

Discussion

Here we used *cis* P-tau mAbs to demonstrate the presence of, and specifically eliminate, pathogenic *cis* P-tau in clinically relevant *in vitro* and *in vivo* models of sport- and military-related TBI. We detected robust *cis* P-tau signals after sport- and military-related TBI in humans and mice, and in stressed neurons. Following TBI or

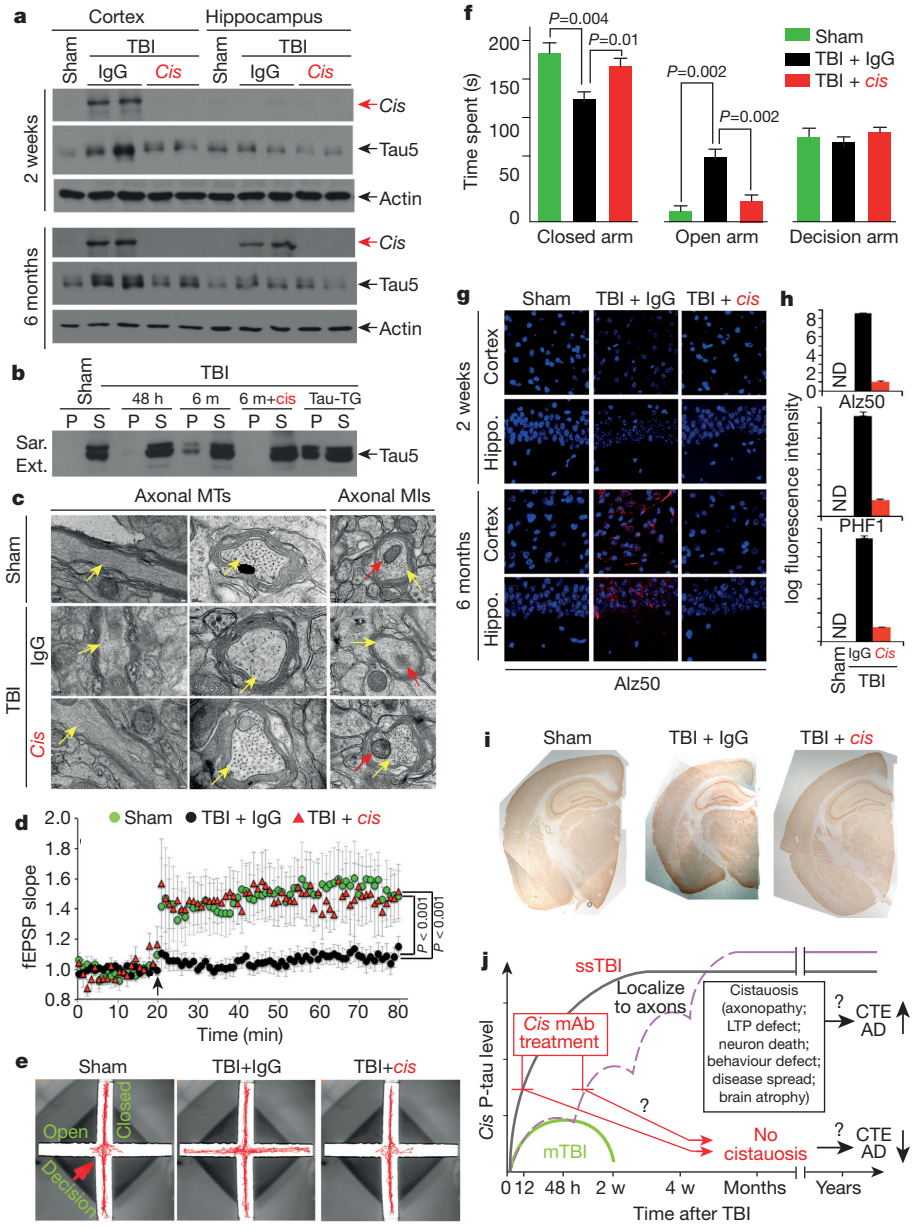

Figure 5 | Treating ssTBI mice with *cis* mAb blocks early cistauosis, prevents tauopathy development and spread, and improves histopathological and functional outcomes. **a**, **b**, ssTBI mice were treated with *cis* mAb or control IgG for times indicated, along sham mice as controls, followed by immunoblotting to detect *cis* P-tau (**a**), and sarcosyl extraction to detect tau aggregation (**b**). TG, transgenic; $n = 4$. **c**, **d**, After 2 week's treatment, ssTBI mice were subjected to electron microscopy for axonal structures of microtubules (yellow arrows) and mitochondrias (red arrows) (**c**) or cortical fSPSP recording (**d**) (mean ± s.e.m.). Black arrow, theta-burst application; $n = 15$ slices from 9 sham; $n = 9$ slices from 5 IgG or *cis* mAb mice. *P* values, one-way ANOVA with Bonferroni post hoc test. **e**, **f**, After 2 month's treatment, ssTBI mice were subjected to the elevated plus maze (**e**) and time spent in three arms was measured (**f**) (mean ± s.e.m.). $n = 4$ for sham; $n = 7$ for IgG or *cis* mAb. *P* values, Student's *t*-test. **g**, **h**, After 2 week's or 6 month's treatment, ssTBI mice were subjected to immunofluorescence with tauopathy mAbs (**g**), with quantification in the hippocampus being shown (**h**) (means ± s.d.). $n = 4$. **i**, After 6 month's treatment, ssTBI mice were immunostained with NeuN before determining brain thickness. $n = 4$. **j**, Unlike single mTBI, rmTBI or ssTBI causes robust and persistent *cis* P-tau induction within 12–24 h post-injury, which induces cistauosis, long before commonly known tauopathy and brain atrophy, hallmarks of CTE and Alzheimer's disease. *Cis* mAb not only blocks early cistauosis, but also prevents long-term neurodegeneration after TBI.

neuronal stress, *cis* P-tau induces cistauosis well before previously identified tauopathy is apparent. Treating TBI mice with *cis* mAb ablates *cis* P-tau and eliminates cistauosis, prevents the development of widespread tauopathy and restores histopathological and many functional outcomes of TBI. Cistausosis is an early precursor of previously described tauopathy and an early marker of neurodegeneration that can be blocked by *cis* mAb. We previously showed that *cis* P-tau has an early pathological role in Alzheimer's disease[27–34,42]. Our current data provide a direct link from TBI to CTE and Alzheimer's disease, and suggest that cistauosis is a common early disease mechanism in TBI, CTE and Alzheimer's disease, and that *cis* P-tau and its mAb may be useful for early diagnosis, prevention and therapy for these devastating diseases (Fig. 5j).

Online Content Methods, along with any additional Extended Data display items and Source Data, are available in the online version of the paper; references unique to these sections appear only in the online paper.

Received 17 June 2014; accepted 11 June 2015.
Published online 15 July 2015.

1. Faul, M., Xu, L., Wald, M. M. & Coronado, V. G. Traumatic brain injury in the United States: emergency department visits, hospitalizations, and deaths, 2002–2006. http://www.cdc.gov/traumaticbraininjury/tbi_ed.html (Centers for Disease Control and Prevention, 2010).
2. Centers for Disease Control and Prevention. CDC grand rounds: reducing severe traumatic brain injury in the United States. *MMWR Morb. Mortal. Wkly Rep.* **62,** 549–552 (2013).
3. Tanielian, T. *et al.* Invisible wounds of war: psychological and cognitive injuries, their consequences, and services to assist recovery. http://www.rand.org/pubs/monographs/MG720 (RAND Corporation, 2008).
4. Omalu, B. I. *et al.* Chronic traumatic encephalopathy in a National Football League player. *Neurosurgery* **57,** 128–134 (2005).
5. Goldstein, L. E. *et al.* Chronic traumatic encephalopathy in blast-exposed military veterans and a blast neurotrauma mouse model. *Sci. Transl. Med.* **4,** 134ra160 (2012).
6. McKee, A. C. *et al.* The spectrum of disease in chronic traumatic encephalopathy. *Brain* **136,** 43–64 (2013).
7. Smith, D. H., Johnson, V. E. & Stewart, W. Chronic neuropathologies of single and repetitive TBI: substrates of dementia? *Nature Rev. Neurol.* **9,** 211–221 (2013).
8. DeKosky, S. T., Blennow, K., Ikonomovic, M. D. & Gandy, S. Acute and chronic traumatic encephalopathies: pathogenesis and biomarkers. *Nature Rev. Neurol.* **9,** 192–200 (2013).
9. Blennow, K., Hardy, J. & Zetterberg, H. The neuropathology and neurobiology of traumatic brain injury. *Neuron* **76,** 886–899 (2012).
10. Mortimer, J. A. *et al.* Head trauma as a risk factor for Alzheimer's disease: a collaborative re-analysis of case-control studies. EURODEM Risk Factors Research Group. *Int. J. Epidemiol.* **20** (Suppl. 2), S28–S35 (1991).
11. Guo, Z. *et al.* Head injury and the risk of AD in the MIRAGE study. *Neurology* **54,** 1316–1323 (2000).

12. Nordström, P., Michaelsson, K., Gustafson, Y. & Nordström, A. Traumatic brain injury and young onset dementia: a nationwide cohort study. *Ann. Neurol.* **75,** 374–381 (2014).
13. Ballatore, C., Lee, V. M. & Trojanowski, J. Q. Tau-mediated neurodegeneration in Alzheimer's disease and related disorders. *Nature Rev. Neurosci.* **8,** 663–672 (2007).
14. Mandelkow, E. M. & Mandelkow, E. Biochemistry and cell biology of tau protein in neurofibrillary degeneration. *Cold Spring Harb. Perspect. Med.* **2,** a006247 (2012).
15. Clavaguera, F. *et al.* Transmission and spreading of tauopathy in transgenic mouse brain. *Nature Cell Biol.* **11,** 909–913 (2009).
16. de Calignon, A. *et al.* Propagation of tau pathology in a model of early Alzheimer's disease. *Neuron* **73,** 685–697 (2012).
17. Liu, L. *et al.* Trans-synaptic spread of tau pathology *in vivo*. *PLoS ONE* **7,** e31302 (2012).
18. Clavaguera, F. *et al.* Peripheral administration of tau aggregates triggers intracerebral tauopathy in transgenic mice. *Acta Neuropathol.* **127,** 299–301 (2014).
19. Clavaguera, F., Hench, J., Goedert, M. & Tolnay, M. Invited review: prion-like transmission and spreading of tau pathology. *Neuropathol. Appl. Neurobiol.* **41,** 47–58 (2015).
20. Asuni, A. A., Boutajangout, A., Quartermain, D. & Sigurdsson, E. M. Immunotherapy targeting pathological tau conformers in a tangle mouse model reduces brain pathology with associated functional improvements. *J. Neurosci.* **27,** 9115–9129 (2007).
21. Rosenmann, H. Immunotherapy for targeting tau pathology in Alzheimer's disease and tauopathies. *Curr. Alzheimer Res.* **10,** 217–228 (2013).
22. Sigurdsson, E. M. Tau immunotherapy and imaging. *Neurodegener. Dis.* **13,** 103–106 (2014).
23. Smith, C., Graham, D. I., Murray, L. S. & Nicoll, J. A. Tau immunohistochemistry in acute brain injury. *Neuropathol. Appl. Neurobiol.* **29,** 496–502 (2003).
24. Johnson, V. E., Stewart, W. & Smith, D. H. Widespread tau and amyloid-beta pathology many years after a single traumatic brain injury in humans. *Brain Pathol.* **22,** 142–149 (2012).
25. Mannix, R. *et al.* Clinical correlates in an experimental model of repetitive mild brain injury. *Ann. Neurol.* **74,** 65–75 (2013).
26. Lu, K. P., Hanes, S. D. & Hunter, T. A human peptidyl-prolyl isomerase essential for regulation of mitosis. *Nature* **380,** 544–547 (1996).
27. Lu, P. J., Wulf, G., Zhou, X. Z., Davies, P. & Lu, K. P. The prolyl isomerase Pin1 restores the function of Alzheimer-associated phosphorylated tau protein. *Nature* **399,** 784–788 (1999).
28. Zhou, X. Z. *et al.* Pin1-dependent prolyl isomerization regulates dephosphorylation of Cdc25C and tau proteins. *Mol. Cell* **6,** 873–883 (2000).
29. Liou, Y.-C. *et al.* Role of the prolyl isomerase Pin1 in protecting against age-dependent neurodegeneration. *Nature* **424,** 556–561 (2003).
30. Pastorino, L. *et al.* The prolyl isomerase Pin1 regulates amyloid precursor protein processing and amyloid-beta production. *Nature* **440,** 528–534 (2006).
31. Lu, K. P. & Zhou, X. Z. The prolyl isomerase PIN1: a pivotal new twist in phosphorylation signalling and human disease. *Nature Rev. Mol. Cell Biol.* **8,** 904–916 (2007).
32. Lim, J. *et al.* Pin1 has opposite effects on wild-type and P301L tau stability and tauopathy. *J. Clin. Invest.* **118,** 1877–1889 (2008).
33. Lee, T. H., Pastorino, L. & Lu, K. P. Peptidyl-prolyl cis-trans isomerase Pin1 in aging, cancer and Alzheimer's disease. *Expert Rev. Mol. Med.* **13,** e21 (2011).
34. Driver, J. A., Zhou, X. Z. & Lu, K. P. Pin1 dysregulation helps to explain the inverse association between cancer and Alzheimer's disease. *Biochim. Biophys. Acta*. http://dx.doi.org/10.1016/j.bbagen.2014.12.025 (2015).
35. Chen, C. H. *et al.* Pin1 cysteine-113 oxidation inhibits its catalytic activity and cellular function in Alzheimer's disease. *Neurobiol. Dis.* **76,** 13–23 (2015).
36. Lee, T. H. *et al.* Death associated protein kinase 1 phosphorylates Pin1 and inhibits its prolyl isomerase activity and cellular function. *Mol. Cell* **42,** 147–159 (2011).
37. Kim, B. M. *et al.* Death-associated protein kinase 1 has a critical role in aberrant tau protein regulation and function. *Cell Death Dis.* **5,** e1237 (2014).
38. Ma, S. L. *et al.* A PIN1 polymorphism that prevents its suppression by AP4 associates with delayed onset of Alzheimer's disease. *Neurobiol. Aging* **33,** 804–813 (2012).
39. Wijsman, E. M. *et al.* Evidence for a novel late-onset Alzheimer disease locus on chromosome 19p13.2. *Am. J. Hum. Genet.* **75,** 398–409 (2004).
40. Luna-Muñoz, J., Chavez-Macias, L., Garcia-Sierra, F. & Mena, R. Earliest stages of tau conformational changes are related to the appearance of a sequence of specific phospho-dependent tau epitopes in Alzheimer's disease. *J. Alzheimers Dis.* **12,** 365–375 (2007).
41. Hampel, H. *et al.* Total and phosphorylated tau protein as biological markers of Alzheimer's disease. *Exp. Gerontol.* **45,** 30–40 (2010).
42. Nakamura, K. *et al.* Proline isomer-specific antibodies reveal the early pathogenic tau conformation in Alzheimer's disease. *Cell* **149,** 232–244 (2012).
43. Lasagna-Reeves, C. A. *et al.* Identification of oligomers at early stages of tau aggregation in Alzheimer's disease. *FASEB J.* **26,** 1946–1959 (2012).
44. Johnson, V. E., Stewart, W. & Smith, D. H. Axonal pathology in traumatic brain injury. *Exp. Neurol.* **246,** 35–43 (2013).
45. Congdon, E. E., Gu, J., Sait, H. B. & Sigurdsson, E. M. Antibody uptake into neurons occurs primarily via clathrin-dependent Fcγ receptor endocytosis and is a prerequisite for acute tau protein clearance. *J. Biol. Chem.* **288,** 35452–35465 (2013).
46. Mallery, D. L. *et al.* Antibodies mediate intracellular immunity through tripartite motif-containing 21 (TRIM21). *Proc. Natl Acad. Sci. USA* **107,** 19985–19990 (2010).
47. Cruz, J. C., Tseng, H. C., Goldman, J. A., Shih, H. & Tsai, L. H. Aberrant Cdk5 activation by p25 triggers pathological events leading to neurodegeneration and neurofibrillary tangles. *Neuron* **40,** 471–483 (2003).
48. Williams, S. *et al.* In situ DNA fragmentation occurs in white matter up to 12 months after head injury in man. *Acta Neuropathol.* **102,** 581–590 (2001).
49. Adhikari, A., Topiwala, M. A. & Gordon, J. A. Single units in the medial prefrontal cortex with anxiety-related firing patterns are preferentially influenced by ventral hippocampal activity. *Neuron* **71,** 898–910 (2011).
50. Schwarzbold, M. L. *et al.* Effects of traumatic brain injury of different severities on emotional, cognitive, and oxidative stress-related parameters in mice. *J. Neurotrauma* **27,** 1883–1893 (2010).

Supplementary Information is available in the online version of the paper.

Acknowledgements We thank T. Hunter and M. Zeidel for advice; S. Hagen for Microscopy Facility (NIH grant S10 RR017927) and P. Davies for tauopathy antibodies. C.-H.C., Y.-M.L., J.A.D. and S.W. are recipients of NIA-funded T32 Translational Research in Aging Training Grant, National Science Council Postdoctoral Fellowship from Taiwan, a VA Career Development Award, and Susan G. Komen postdoctoral fellowship, respectively. R.M. is supported by Boston Children's Hospital Pilot Grant Award and NIH training grant T32HD040128, and A.P.-L. and W.M. by NFLPA. The CTE and blast samples used are supported by grants from NIH (U01NS086659-01, P30AG13846), VA, Sports Legacy Institute, Andlinger Foundation, NFL and WWE. The work is supported by NIH grants R01AG029385, R01CA167677, R01HL111430 and R01AG046319, and Alzheimer's Association grant DVT-14-322623 to K.P.L. and BIDMC and NFLPA pilot grants to K.P.L. and X.Z.Z.

Author Contributions A.K. and K.S. designed the studies, performed the experiments, and wrote the manuscript; R.M. helped design and conduct experiments and analysed the data on impact TBI mouse models and wrote the manuscript; J.Q. and W.M. helped with impact TBI experiments, J.M. and L.E.G. helped with blast TBI experiments and edited the manuscript; A.C.M. provided human brains and edited the manuscript; Y.S. and A.Ro. performed field excitatory postsynaptic potential (fSPSP) recording; C.-H.C., Y.Y., Y.-M.L, J.A.D., S.W., M.-L.L., O.A. and P.H. provided technical assistance; A.Ry. provided assistance for developing mAbs; A.P.-L. advised the project; X.Z.Z. originally discovered the procedures for generating *cis* and *trans* antibodies; and X.Z.Z. and K.P.L. conceived and supervised the project, designed the studies, analysed the data, and wrote the manuscript.

Author Information Reprints and permissions information is available at www.nature.com/reprints. The authors declare competing financial interests: details are available in the online version of the paper. Readers are welcome to comment on the online version of the paper. Correspondence and requests for materials should be addressed to K.P.L. (klu@bidmc.harvard.edu) or X.Z.Z. (xzhou@bidmc.harvard.edu).

METHODS

Mouse mAb production. *Cis* and *trans* mouse mAbs were produced using the general strategy that we used to generate polyclonal *cis* and *trans* antibodies, as described[42]. Briefly, Balb/c female mice (2–3 months old) obtained from the Jackson Laboratories (Bar Harbour, ME) were immunized with 100 μg of pThr231-Homoproline (pThr231-Pip) tau peptide (CKKVAVVRpT(Pip) PKSPSSAK) that was coupled to KLH with N-terminal Cys mixed with complete Freund's adjuvant and boosted twice. The titration of antibody production was monitored using ELISA. When sufficient titration of antibody was produced, splenocytes were isolated and fused with SP2/0 myeloma cells to produce hybridoma cell lines, followed by screening for positive clones using ELISA for *cis* and *trans* mAbs. When positive clones were identified, they were subcloned by a limited dilution to generate single pure clones. mAbs were produced by injecting 2 ml of 2.5×10^6 cells per ml hybridoma cells into nude mice intraperitoneally to collect ascites, followed by purifying mAbs from ascites using antibody purification kit (Pierce) and their specificity were fully characterized. All these animal experiments were approved by Beth Israel Deaconess Medical Center IACUC and complied with the NIH Guide for the Care and Use of Laboratory Animals.

ELISA assays. ELISA assays were performed using wild-type phosphorylated Thr231-Pro tau (KVAVVRpTPPKSPS), non-phosphorylated Thr231 tau (KVAVVRTPPKSPS), *cis* locked phosphorylated Thr231-Dmp tau (KVAVV RpT(5,5-dimethyl-L-proline)PKSPS) and *trans* lock phosphorylated Thr231-Ala tau (P232A)(KVAVVRpTAPKSPS) peptides, as described[42]. Briefly, peptides at various concentrations in 2,2,2-trifluoroethanol (50 μl) were plated onto maxi soap ELISA plate and dried up at 37 °C overnight. After blocking with buffer containing 5% milk, 0.4% bovine serum albumin and 0.05% Tween 20 in Tris-buffered saline, the *cis* or *trans* mAbs at various dilutions in 5% milk, 0.4% bovine serum albumin and 0.05% Tween 20 in Tris-buffered saline (50 μl) was loaded and incubated at room temperature for 2 h, followed by incubation with horseradish peroxidase (HRP)-conjugated anti-rabbit IgG in 5% milk, 0.4% bovine serum albumin and 0.05% Tween 20 in Tris-buffered saline (50 μl) for 1 h. The ELISA plates were washed 4 times with buffer containing 0.4% BSA and 0.05% Tween 20 in TBS after each step. The signals were detected by incubating with TMB substrate solution and were measured by Wallac 1420 software at 450 nm.

Surface plasmon resonance. Surface plasmon resonance experiments were performed on a BIAcore 3000 surface plasmon resonance instrument (GE Healthcare-BIAcore) as described by the manufacturer. Briefly, Biacore sensor chip CM-5 was activated by using EDC (1-ethyl-3-(3-dimethylaminopropyl)-carbodiimide) and NHS (*N*-hydroxysuccinimide) in a 1:1 ratio for 7 min. Anti-mouse IgG (Fc) (GE healthcare) was immobilized at pH 5 on flow cells 1 and 2, followed by the capture of 3.7 μg ml^{-1} of *cis* or *trans* mAb in 10 mM sodium acetate with a flow rate of 5 μl min^{-1}. Then all tau peptides were injected at different concentrations in filtered, degassed 0.01 M HEPES buffer, 0.15 M NaCl, 0.005% surfactant P20, pH 7.4 at a flow rate of 50 μl min^{-1} for 3 min on both flow cells 1 and 2 and allowed to dissociate for 10 min. All samples were run in duplicate. After each run with a single antibody concentration, the surface was totally regenerated by10 mM glycine pH 1.7 flow late 10 μl min^{-1} for 5 s. Data analysis was performed by using BIAevaluation software (GE healthcare-BIAcore).

Immunoblotting analysis and immunodepletion experiment. Immunoblotting analysis was carried out as described[42]. Briefly, brain tissues or culture cells were lysed in RIPA buffer (50 mM Tris-HCl, pH 7.4, 150 mM NaCl, 2 mM EDTA, 1% NP 40, 0.1% SDS, 0.5% Na-deoxycholate, 50 mM NaF) containing proteinase inhibitors and then mixed with the SDS sample buffer and loaded onto a gel after boiling. The proteins were resolved by polyacrylamide gel electrophoresis and transferred to PVDF membrane. After blocking with 5% milk in TBST (10 mM Tris-HCl pH 7.6, 150 mM NaCl, 0.1% Tween 20) for 1 h, the membrane was incubated with primary antibodies (*cis* and *trans* mAbs), Tau5 (Biosource Camarillo, CA), α-tubulin (Sigma, St. Louis, MO) and β-actin antibodies (Sigma, St Louis, MO) in 5% milk in TBST overnight at 4 °C. Then, the membranes were incubated with HRP-conjugated secondary antibodies in 5% milk in TBST. The signals were detected using chemiluminescence reagent (Perkin Elmer, San Jose, CA). The membranes were washed 4 times with TBST after each step. To deplete *cis* or *trans* P-tau from lysates, brain or cell lysates were mixed with the *cis* or *trans* mAb antibody at 425 μg ml^{-1} in RIPA buffer containing proteinase inhibitors for 3 h at 4 °C and then mixed with protein A/G Sepharose for 1 h at 4 °C, followed by collecting the supernatants for experiments. The supernatants were dialysed against phosphate buffer saline (137 mM NaCl, 2.7 mM KCl, 10 mM Na_2HPO_4, 1.8 mM KH_2PO_4) overnight before cell culture application. Immunoblotting results were quantified using Quantity One from BioRad.

Sarkosyl extraction. Isolation of sarkosyl-insoluble and soluble fractions of cells and brain tissues was performed as described[29,32,42], with slight modifications. Briefly, whole brains of mice were homogenized by polytron in 10 volumes of buffer H (10 mM Tris-HCl (pH 7.5) containing 0.8 M NaCl, 1 mM EGTA, and 1 mM dithiothreitol). The cell extraction was also performed with a convenient amount of buffer H (200 μl per 35 mm culture dish) and sonication. The samples were spun at 100,000*g* for 30 min at 4 °C. Another 2 ml of buffer H was added to the pellet and the samples were homogenized again by polytron, incubated in 1% Triton X-100 at 37 °C for 30 min. Following the incubation, the samples were spun at 100,000*g* for 30 min at 4 °C, the pellet was homogenized by polytron on 1 ml of buffer H and was then incubated in 1% sarkosyl at 37 °C for 30 min and spun at 100,000*g* for 30 min at 4 °C. The supernatant was then collected (sarkosyl-soluble fraction). Detergent-insoluble pellets were extracted in 100 μl of urea buffer (8 M urea, 50 mM Tris-HCl (pH 7.5)), sonicated, and spun at 100,000*g* for 30 min at 4 °C. The supernatant was then collected (sarkosyl-insoluble fraction). The protein concentrations of extracts were determined by BCA assay (Thermo Scientific). Sarkosyl-insoluble and -soluble fractions were run on SDS–PAGE gels.

Immunostaining analysis. The primary antibodies used were *cis* and *trans* mAb, tau tangle-related mAbs AT180, AT8, AT100 (all from Innogenetics, Alpharetta, GA), oligomeric tau T22 polyclonal antibodies (EMD Millipore, Billerica, MA), PHF1 and Alz50 (gifts from P. Davies), anti-tau rabbit mAb (E178, Abcam) and anti-neurofilament mouse mAb (SMI-312, IgG1, Abcam) for labelling axons, and anti-MAP2 mAb (SMI-52, IgG1, Abcam) for labelling dendrites. Immunofluorescence staining of mouse and human brains was done essentially as described[29,32,42]. After treatment with 0.3% hydrogen peroxide, slides were briefly boiled in 10 mM sodium citrate, pH 6.0, for antigen enhancement. The sections were incubated with primary antibodies overnight at 4 °C. Then, biotin-conjugated secondary antibodies (Jackson ImmunoResearch), streptavidin-conjugated HRP (Invitrogen) were used to enhance the signals. For double immunofluorescence staining, the sections were also incubated with and Alexa Fluor 488 or 568 conjugated isotype-specific secondary antibodies (Jackson ImmunoResearch, West Grove, PA) for 1 h at room temperature. Manufacturer-supplied blocking buffer (Invitrogen) was used for each reaction. The sections were washed 4 times with TBS after each step. Labelled sections were visualized with a Zeiss confocal microscope. The gain of confocal laser was set at the level where there are no fluorescence signals including autofluorescence in sections without primary antibody but with secondary antibody. Immunostaining images and their colocalization were quantified using Volocity 6.3 from Perkin Elmer and Fiji/ImagJ Coloc 2, respectively.

Electronic microscopy. Sham and TBI mouse models treated with either control IgG or *cis* mAb were perfused with a fixative solution, a mixture of 15% picric acid (13% saturated solution; Sigma, St. Louis, MO, USA), 4% paraformaldehyde (Electron Microscopy Sciences, Hatfield, PA, USA), and 0.1% glutaraldehyde (electron microscopy grade 50% solution; Electron Microscopy Sciences) dissolved in PEM buffer (0.1 M PIPES, pH 7.2, 1 mM EGTA, 1 mM $MgCl_2$). Perfused brains were removed, sliced and kept in the same fixative for further 4 h at 4 °C. The samples were processed for electron microscopic observation as described[51,52]. Specimens were examined with a JEM-1010 transmission electron microscope (JEOL). For immunogold staining, SY5Y cells were treated with *cis* mAb for 18 h, trypsinized and collected by centrifugation, followed by fixation with 4% PFA. Samples were dehydrated with ethanol, processed for LR white resin embedding and sectioning, followed by gold staining as described[53].

Human brain specimens. Fixed human brain tissue from the frontal cortex of individuals with neuropathologically verified CTE was provided from the VA-BU-SLI Brain Bank of the Boston University Alzheimer's Disease Center CTE Program, including 16 patients with a history of exposure to TBI and 8 age-matched healthy controls (Supplementary Table 1)[6]. Next of kin provided written consent for participation and brain donation. Institutional review board approval for brain donation was obtained through the Boston University Alzheimer's Disease Center, CTE Program, and the Bedford VA Hospital. Institutional review board approval for neuropathological evaluation was obtained through Boston University School of Medicine[6]. Our studies on human samples have been approved by our Institutional Review Boards at Boston University and Beth Israel Deaconess Medical Center

Transgenic overexpression and knockout mice. Tau-transgenic mice[54] and tau-knockout mice[55] (Jackson laboratory) in the C57BL/6 background were generated, as described[29,32,42]. Animal care and use for the experiments have been approved by Institutional Animal Care and Use Committees at Beth Israel Deaconess Medical Center.

Cell culture. Neuronal cell lines including SH-SY5Y, PC12, H4 cells (purchased originally from American Type Culture Collection) were cultured in Dulbecco's modified Eagle's medium (DMEM) containing 10% fetal calf serum. The cell lines have not been authenticated or tested for mycoplasma contamination. The media were supplemented with 100 Units ml^{-1} penicillin/streptomycin. PC12 cells were differentiated with NGF (50 ng ml^{-1}) and cultured for 2 days before stress. SY5Y

cells (2.5×10^5 per ml) were transiently co-transfected with 2.5 μg GFP–tau, 2.5 μg Cdk5 and 2.5 μg p25 with Lipofectamine 2000 (Invitrogen) as described[40]. Cells were treated with *cis* or *trans* mAbs at 8.0 μg ml^{-1} once 4 h after transfection until observation.

Cell viabilities were examined using Live & Dead cell assay kit (Abcam) according to the manufacturer. For apoptosis assay, cells were trypsinized and suspended in a binding buffer (10 mM HEPES, pH 7.4; 140 mM NaCl; 2.5 mM $CaCl_2$), stained with Annexin V (Biolegend 640912) for 15 min and subjected for flow cytometry. Brain or cell extracts were applied to culture SY5Y cells for 18 h and the cell viabilities were examined as described earlier. We performed the cell or brain lysate extraction using RIPA buffer but efficiently dialysed the extracts against PBS for 48 h dialysis with 4 changes of buffer.

Stably overexpressing RFP– or GFP–tau SY5Y cells were routinely generated. Briefly, the plasmids pcDNA3.1-tau-RFP and -GFP constructed through restriction sites and were transfected into SY5Y cells via Lipofectamine 2000. Cells stably expressing tau selected with G418). Equal number of GFP– and RFP–tau expressing cells (2.5×10^5 per ml) were cocultured, treated or untreated with either *cis* or *trans* mAbs at concentration of 170 μg ml^{-1} for 18 h before moving into hypoxia chamber.

To test cell or brain lysates, accordingly, we performed the extraction using RIPA buffer but efficiently dialysed the extracts against PBS with a cocktail of protease inhibitors at 4 °C for 48 h dialysis with 4 changes of the buffer. After dialysis, we examined *cis* tau concentration and conformation with immunoblotting and applied the amount of dialysed lysates similar to the original lysates to culture dishes. SY5Y cells were treated with 3-methyladenine at concentration of 5 mM for 24 h.

Primary neurons were prepared from 17-day-old embryonic mouse brain cerebral cortex of either sex. Neurons were seeded on pre-coated culture dishes (2×10^5 per ml). The medium was then changed to neurobasal medium supplemented with B27 (Invitrogen) and 1 mM L-glutamine as described[52]. Neurons were infected with lentivirus coding for either GFP– or RFP–tau for 72 h.

Mitochondrial transport assay. PC12 cells were differentiated with NGF (Cell Signaling) at 50 ng ml^{-1} and cultured for 2 days before stress. They were treated with *cis* or *trans* mAbs at 85 μg ml^{-1} for 18 h and transferred into hypoxia chamber for 48 h more. Then, mitochondria were stained using Mitotracker Green FM (Life technologies) according to manufacturer and observed with a Zeiss confocal microscope for 30 min using an incubation chamber with 5% CO_2 at 37 °C. Fluorescent images of labelled mitochondria in the longest process of each PC12 cell were acquired at intervals of 5 s over a period of 30 min. Individual mitochondrial movements were analysed with ZEN 2008 software (Zeiss). Differences in the position of each mitochondrion between two frames during each 5 s interval were exported to Excel, and they were classified and scored as stationary, fast (>0.05 μm s^{-1}) or slow (<0.05 μm s^{-1}) movements.

Traumatic brain injury. The mouse TBI model was used as previously described[25,56]. Briefly, male C57BL/6 mice (2–3 months old) obtained from the Jackson Laboratories (Bar Harbour, ME) were randomized to undergo injury or sham-injury. The mice were anaesthetized for 45 s using 4% isoflurane in a 70:30 mixture of air:oxygen. Anaesthetized mice were placed on a delicate task wiper (Kimwipe, Kimberly-Clark, Irving, TX) and positioned such that the head was placed directly under a hollow guide tube. The mouse's tail was grasped. A 54-gram metal bolt was used to deliver an impact to the dorsal aspect of the skull, resulting in a rotational acceleration of the head through the Kimwipe. Mice underwent single severe injury (ssTBI, 60-inch height), singe mild injury (mTBI, 28-inch height), or repetitive mild injuries (rmTBI, 7 injuries in 9 days). Sham-injured mice underwent anaesthesia but not concussive injury. All mice were recovered in room air. Anaesthesia exposure for each mouse was strictly controlled to 45 s. Subsequent behavioural and histopathological testing was conducted in a blinded manner. Blast-induced TBI mouse model was performed as described[5]. Briefly, anaesthetized adult wild-type C57BL/6 male mice were exposed to a single blast or sham blast, removed from the apparatus, monitored until recovery of gross locomotor function, and then transferred to their home cage. Maximum burst pressure compatible with 100% survival and no gross motor abnormalities was ascertained empirically. All these and following animal experiments were approved by the Boston Children's Hospital, Beth Israel Deaconess Medical Center and/or Boston University and IACUC and complied with the NIH Guide for the Care and Use of Laboratory Animals.

Antibody treatment of mice. Mice undergoing TBI were randomized to treatment with anti-*cis* P-tau monoclonal mouse antibody or mouse IgG2b. Mice received 1 dose of *cis* antibody or IgG2b intraperitoneal pre-treatment (i.p. 200 μg per mouse) 3 days before the injury (which was omitted in some experiments), post-injury treatment with single intracerebroventricular (ICV) treatment (20 μg in 5 microlitres) 15 min after injury, then post-treatment 200 μg i.p. every 4 days for 3 times and analysed brains 14 days later for immunoblotting or fEPSP recording, followed by 200 μg i.p. weekly for another 1.5 months (with a total 2 months of treatment) before the elevated plus maze or the Morris Water Maze in a double-blinded manner. After the above treatment, some mice received further antibody treatment, by 200 μg i.p. biweekly for another 4 months before assaying *cis* P-tau spread, tau aggregation and tauopathy and brain atrophy at 6 months after ssTBI, as described[29,32,42]. For all behavioural tests, experimenters were blinded to injury and treatment status, using colour-coding stored in a password protected computer.

Electrophysiology. Mice were anaesthetized with isoflurane (NDC 10019-360-40, Baxter Healthcare Corporation Deerfield, IL, USA) and decapitated. The brains were quickly removed and placed for sectioning in ice-cold treatment artificial cerebrospinal fluid (tACSF) containing (in mM) NaCl 124, KCl 3, NaH_2PO_4 1.25, $NaHCO_3$ 26, $CaCl_2$ 2, $MgSO_4$ 2, and glucose 10 (pH 7.4, and bubbled with 95% O_2 and 5% CO_2 gas mixture). Cortical slices (thickness 350 μm) were cut with a Vibratome 1000P (Leica VT1000P, Leica Microsystems Inc., Buffalo Grove, IL, USA) and transferred to a chamber with oxygenated tACSF for 90 min at 30 °C before recording.

Field excitatory postsynaptic potentials (fEPSP) were recorded using a multi-electrode array recording system (MED64 system) with MED-P5155 probe (AutoMate Scientific, Inc., Berkeley, CA, USA) in this study. After incubation, one cortical slice was positioned in the centre of the MED64 probe (to fully cover the 8 × 8 electrode array) with oxygenated recording ACSF (rACSF) containing (in mM) NaCl 124, KCl 3, NaH_2PO_4 1.25, $NaHCO_3$ 26, $CaCl_2$ 2, $MgSO_4$ 1, and glucose 10 (pH 7.4) at 30 °C. A fine nylon mesh and a mesh anchor were placed on top of the slice to immobilize the slice during recording. The probe with immobilized slice was connected to two MED64 amplifiers (MED64 Head Amplifier (MED-A64HE1) and Main Amplifier (MED-A64MD1), AutoMate Scientific, Inc., Berkeley, CA, USA). The slice was continuously perfused with oxygenated, fresh rACSF at the rate of 2 ml min^{-1} using a peristaltic pump (Minipuls 3, Gilson Inc., Middleton, WI).

Data was collected using Mobius software (Mobius 0.4.2). Field potentials were induced by single pulses (0.2 ms) delivered at 0.05 Hz through one planar microelectrode in layer V of cortical slice. We used stimulus intensity sufficient to induce a 50% of the maximal fEPSP slope in all experiments. The fEPSP was recorded from the channels in layer II/III. A stable fEPSP slope for at least 20 min was recorded as baseline. The induction protocol of LTP that we used is 5 Hz theta burst (each burst consists of 4 pulses at 100 Hz). The data were filtered at 10 kHz and digitized at a 20 kHz sampling rate. Data were analysed off line by the MED64 Mobius software. For quantifying the level of LTP, the mean of fEPSP slope (10–40%) within the last 10 min of recording was normalized and expressed as a fold change of the averaged baseline (first 10 min of the baseline). Three successive responses were averaged. Statistics were performed using the number of slices as '*n*' value, and one to two slices per animal. *P* values were calculated using one-way ANOVA with Bonferroni post hoc test.

Morris water maze. A Morris water maze (MWM) paradigm was used to evaluate spatial learning and memory as described[25,57]. Briefly, a white pool (83 cm diameter, 60 cm deep) was filled with water to 29 cm depth. Water temperature was maintained at approximately 24 °C. Several highly visible intra- and extra-maze cues were located in and around the pool. The target platform (a round, clear, plastic platform 10 cm in diameter) was positioned 1 cm below the surface of the water. During hidden and visible platform trials, mice were randomized to one of four starting quadrants. Mice were placed in the tank facing the wall and given 90 s to find the platform, mount the platform, and remain on it for 5 s. Mice were then placed under a heat lamp to dry before their next run. Time until the mouse mounted the platform (escape latency) was measured and recorded. Mice that failed to mount the platform within the allotted time (90 s) were guided to the platform by the experimenter and allowed 10 s to become acquainted with its location. Each mouse was subjected to a maximum of two trials per day, each consisting of four runs, with a 45-min break between trials. For visible platform trials, a red reflector was used to mark the top of the target platform. For probe trials, mice were placed in the tank with the platform removed and given 60 s to explore the tank. Noldus Ethovision 9 software tracked swim speed, total distance moved, and time spent in the target quadrant where the platform was previously located. When mice underwent repeat MWM testing, 2 to 3 months or 6 months after their final injury, the platform was moved to a different quadrant than that used previously.

Elevated plus maze. The elevated plus maze was used to assess anxiety/risk-taking behaviour two months after injury and carried out as described[58]. Briefly, the elevated plus maze consists of two open and two closed arms (30 × 5 cm) extended out opposite from each other from a central platform (decision zone) to create a plus shape. The entire apparatus is raised 85 cm above the floor (Lafayette Instruments). Mice are placed on the centre platform of the maze, facing a closed arm, and allowed to explore the apparatus for

5 min. The maze is cleaned between subjects with a weak ethanol solution and dried. A computer-assisted video-tracking system (Noldus Ethovision) recorded the total time spent in the open centre (decision zone), and the two closed or 'safe' arms and the two open or 'aversive' arms. The percent time spent in the open arms is used as a surrogate measure of anxiety/risk-taking behaviour; mice with lower levels of anxiety/risk-taking behaviour spend less time in the open arms.

Immunohistochemistry. Mice were intracardially perfused with 4% paraformaldehyde at various time points after injury and brains were collected for histopathological outcomes. Serial 20 μm coronal frozen sections from sham and injured brains were cut on a cryostat (Leica) from the anterior frontal lobes through the posterior extent of the dorsal hippocampus. Every 10th section was collected and mounted on slides.

Statistical analysis. Experiments were routinely repeated at least three times, and the repeat number was increased according to effect size or sample variation. We estimated the sample size considering the variation and mean of the samples. No animals or samples were excluded from any analysis. Animals were randomly assigned groups for *in vivo* studies and for mAb treatment experiments in mice, group allocation and outcome assessment were also done in a double blinded manner. For all behavioural tests, experimenters were blinded to injury and treatment status, using colour coding stored in a password protected computer. All data are presented as the means ± s.d. except behavioural tests where data are presented as the means ± s.e.m., followed by determining significant differences using the two-tailed Student's *t* test for quantitative variables or ANOVA test for continuous or three or more independent variables or one-way ANOVA with Bonferroni post hoc test, and significant P values <0.05 are shown.

51. Tokuoka, H. *et al.* Brain-derived neurotrophic factor-induced phosphorylation of neurofilament-H subunit in primary cultures of embryo rat cortical neurons. *J. Cell Sci.* **113,** 1059–1068 (2000).
52. Shahpasand, K. *et al.* Regulation of mitochondrial transport and inter-microtubule spacing by tau phosphorylation at the sites hyperphosphorylated in Alzheimer's disease. *J. Neurosci.* **32,** 2430–2441 (2012).
53. Farah, C. A. *et al.* Tau interacts with Golgi membranes and mediates their association with microtubules. *Cell Motil. Cytoskeleton* **63,** 710–724 (2006).
54. Ishihara, T. *et al.* Age-dependent emergence and progression of a tauopathy in transgenic mice overexpressing the shortest human tau isoform. *Neuron* **24,** 751–762 (1999).
55. Dawson, H. N. *et al.* Inhibition of neuronal maturation in primary hippocampal neurons from tau deficient mice. *J. Cell Sci.* **114,** 1179–1187 (2001).
56. Meehan, W. P. III, Zhang, J., Mannix, R. & Whalen, M. J. Increasing recovery time between injuries improves cognitive outcome after repetitive mild concussive brain injuries in mice. *Neurosurgery* **71,** 885–892 (2012).
57. Walf, A. A. & Frye, C. A. The use of the elevated plus maze as an assay of anxiety-related behavior in rodents. *Nature Protocols* **2,** 322–328 (2007).
58. Morris, R. Developments of a water-maze procedure for studying spatial learning in the rat. *J. Neurosci. Methods* **11,** 47–60 (1984).

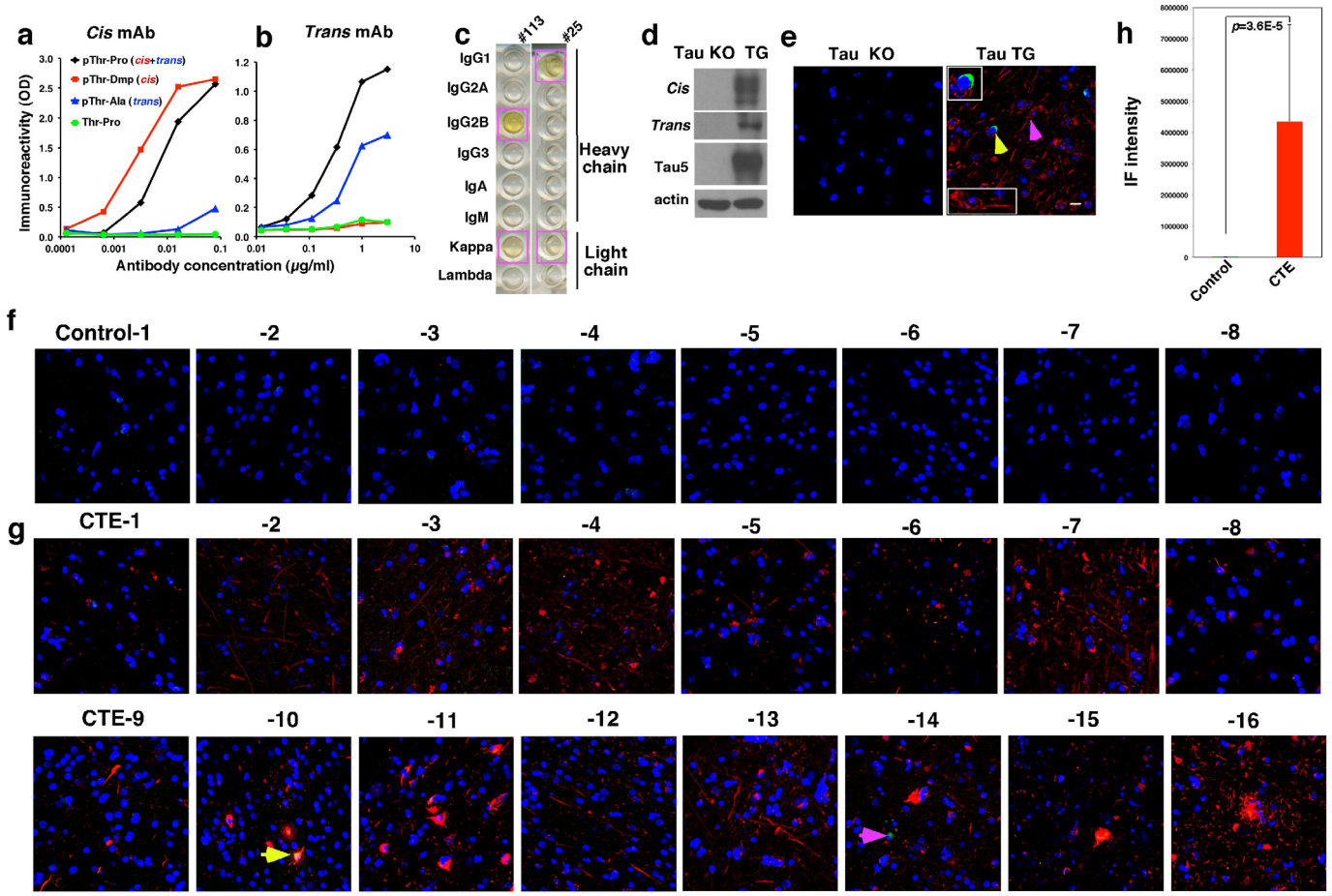

Extended Data Figure 1 | Characterization of *cis* and *trans* P-tau mAbs and robust *cis* P-tau in human CTE brains. **a**, **b**, Characterization of the specificity of *cis* and *trans* P-tau mAbs by ELISA. *Cis* (**a**) and *trans* (**b**) antibodies at various concentrations were incubated with *cis* (pT231-Dmp), *trans* (pT231-Ala), *cis* + *trans* (pT231-Pro) or T231-Pro tau peptides, followed by detecting the binding by ELISA. Representative examples of ELISA are shown from 3 independent experiments. pT231-Pro, CKKVAVVRpT(Pro)PKSPSSAK; pT231-Pip, CKKVAVVRpT(homoproline)PKSPSSAK; pT231-Ala, KVAVVRpT(alanine)PKSPS; pT231-Dmp (KVAVVRpT(5,5-dimethyl-L-proline)PKSPS). **c**, Determination of the isotypes of *cis* and *trans* P-tau mAbs. Isotypes of *cis* and *trans* mAb heavy and light chains were determined by ELISA assay using a commercially available assay kit. **d**, **e**, Characterization of the specificity of *cis* and *trans* P-tau mAbs by immunoblotting and immunofluorescence. Brain lysates (**d**) or sections (**e**) prepared from tau-deficient (KO) or wild-type tau-overexpressing (TG) mice were subjected to immunoblotting or immunofluorescence with *cis* and/or *trans* antibody. The *cis* and *trans* signals were readily detected in TG, but not at all in KO mouse brains, with *cis* in the soma and neurites (pink arrow), but *trans* only in the soma (yellow arrow) (insets). Similar results were observed in at least three different animals. *Cis*, red; *trans*, green; DNA, blue. **f**–**h**, Robust *cis* P-tau in human CTE brains. 16 CTE brain tissues and 8 healthy controls were subjected to immunofluorescence, with one representative image from each case being shown) (**f**, **g**). Yellow arrow points to a neuron expressing both *cis* (red) and *trans* (green) P-tau, while pink one to a neuron expressing only trans in the soma. Fluorescence immunostaining intensity of *cis* P-tau was quantified using Volocity 6.3 from Perkin Elmer (**h**). The results are expressed as means ± s.d. and *P* values determined using the Student's *t*-test.

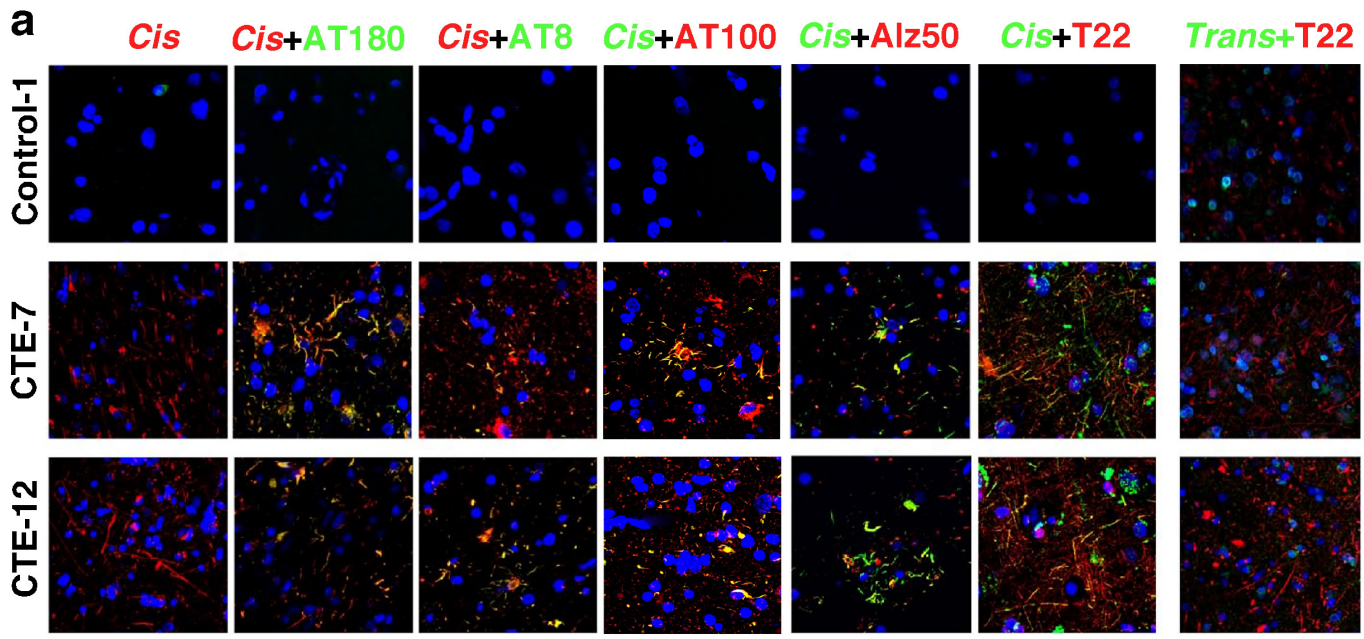

b

	Cis+AT180	*Cis*+AT8	*Cis*+AT100	*Cis*+Alz50	*Cis*+T22	*Trans*+T22
Control	N.D.	N.D.	N.D.	N.D.	N.D.	N.D.
CTE	81.8 ± 6.0	81.2 ± 3.0	80.5 ± 3.6	89.4 ± 7.2	59.0 ± 7.5	0.5 ± 0.4

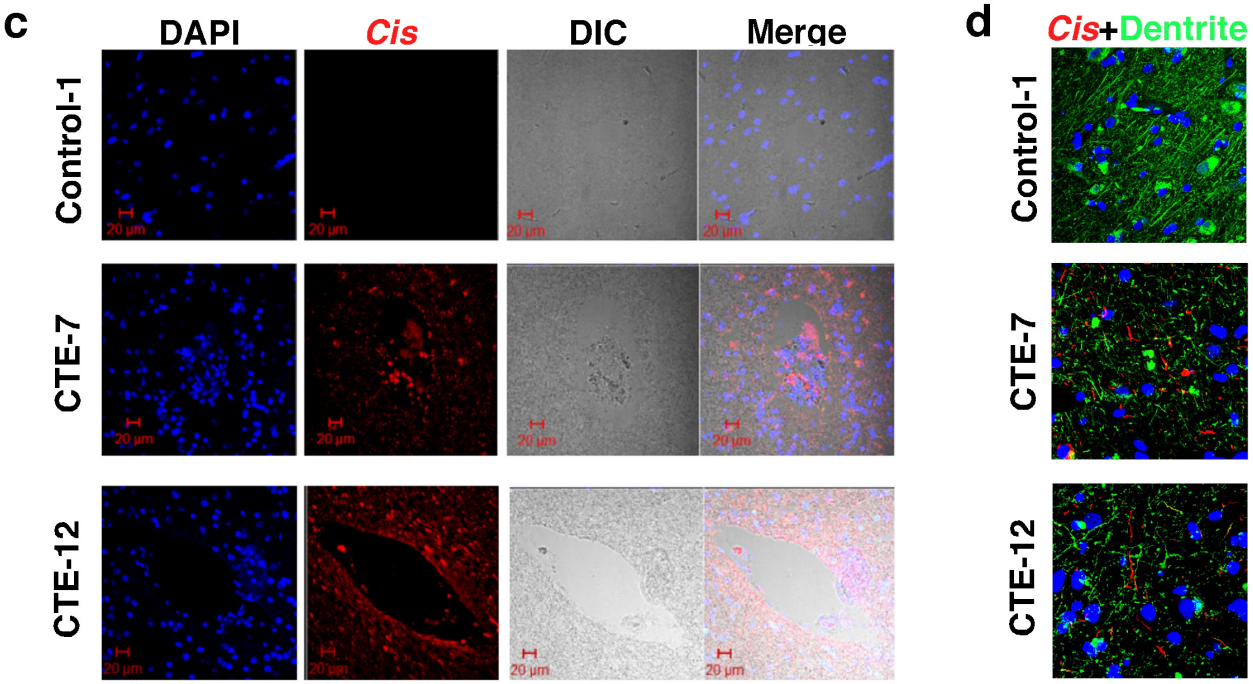

Extended Data Figure 2 | Colocalization of *cis* P-tau with other tau epitopes and its concentration near blood vessels in CTE brains. **a**, **b**, Colocalization of *cis* P-tau with other tau epitopes in CTE brains. CTE brain tissues and healthy controls were stained with *cis* mAb and AT180, AT8, AT100, Alz50 or T22 antibodies, or *trans* mAb and T22 antibodies, with two examples being shown (**a**), and then quantified their colocalization using Coloc 2, with the results being expressed in a percentage (mean ± s.d.) (**b**). N.D., not detectable. **c**, CTE brain tissues and healthy controls were stained with *cis* mAb, with two examples being shown. *Cis* is more prominent near blood vessels, which corresponds to the typical perivascular distribution of P-tau in CTE. **d**, CTE brain tissues and healthy controls were stained with *cis* mAb (red) and the dendritic marker MAP2 (green), along with DNA dye (blue). Colours in the text correspond to their fluorescence labels. $n = 4$.

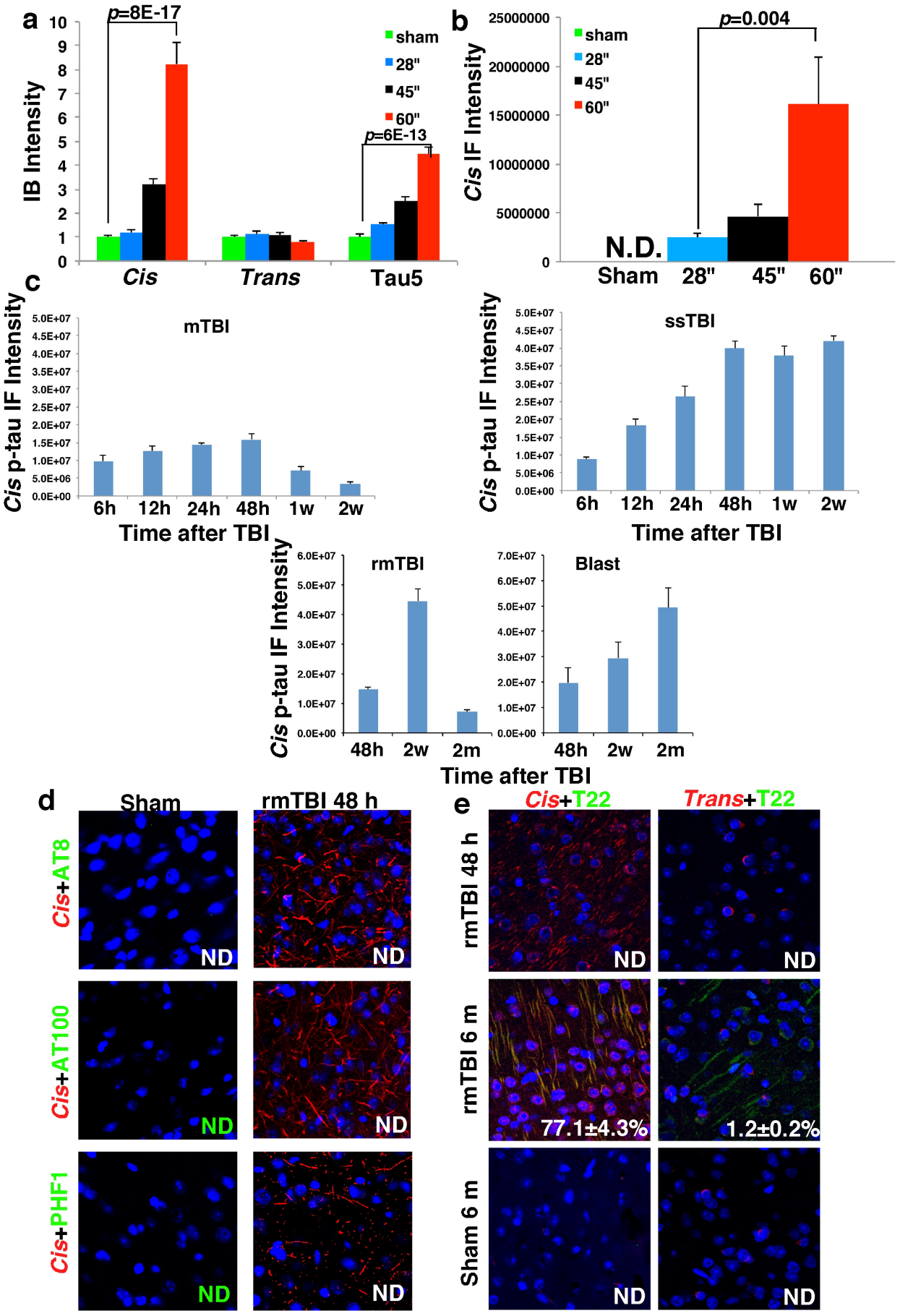

Extended Data Figure 3 | TBI induces *cis* P-tau in a severity- and time-dependent manner long before other known tauopathy epitopes. **a–c**, Severity- and time-dependent induction of *cis* P-tau after TBI. Quantification results of Fig. 2a–f. **d**, Robust *cis* P-tau signals are detected in neurons 48 h after rmTBI without any other tangle-related tau epitopes. 48 h after rmTBI, brain sections were stained with *cis* mAb (red) and AT8, AT100 or PHF1 (green). **e**, Robust *cis* P-tau signals are detected in neurons 48 h after rmTBI without tau oligomerization, which appear and colocalize with *cis* P-tau at 6 months after TBI. 48 h or 6 months after rmTBI or sham treatment, brain sections were immunostained with T22 (green) and *cis* or *trans* mAb (red). The results in 48 h sham mice were similar to those at 6 months (data not shown). The colocalization of red and green signals was quantified using Coloc-2, with the results being shown in percentages. ND, not detectable. $n = 3–4$. The results are expressed as means ± s.d. and P values determined using the Student's t-test.

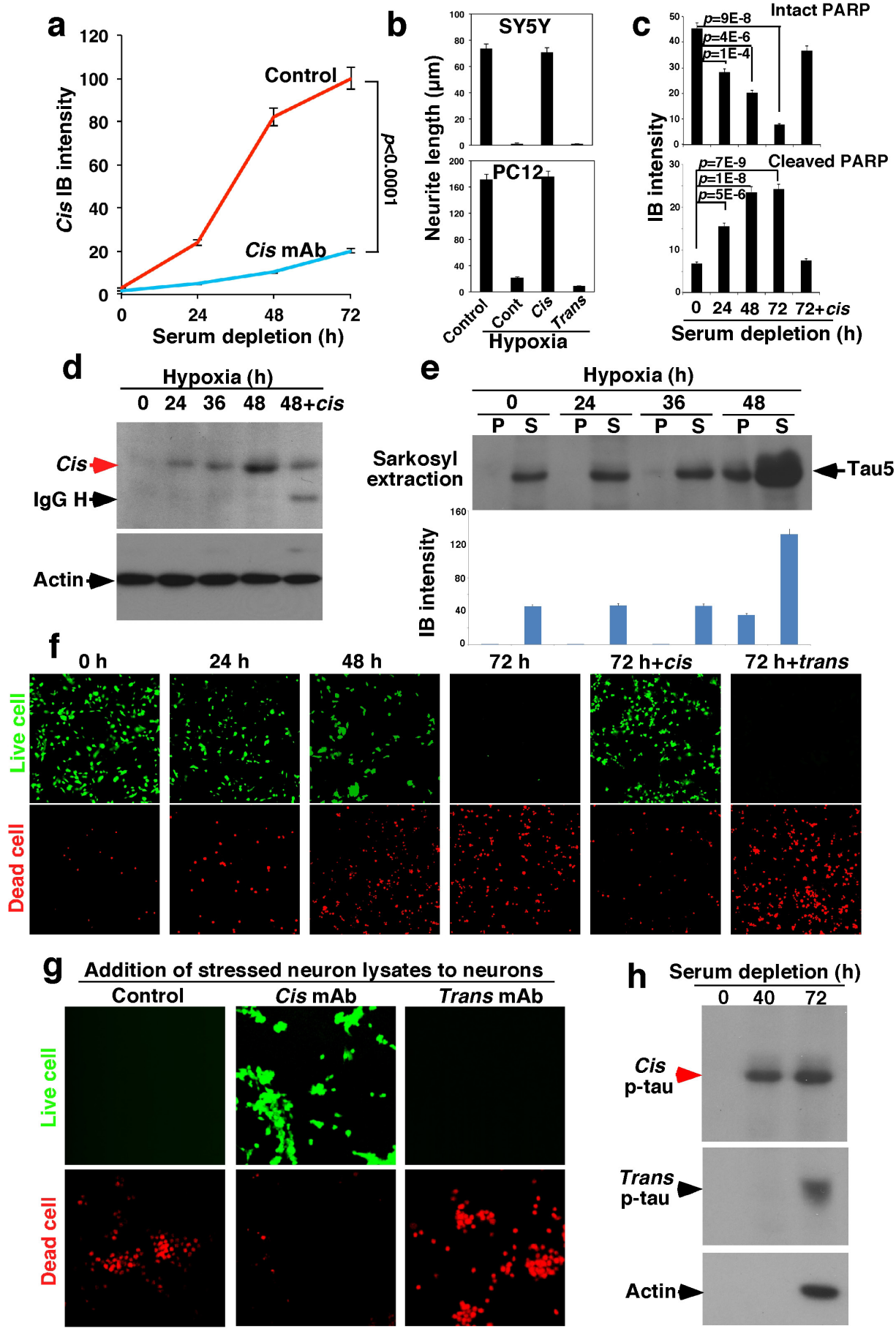

Extended Data Figure 4 | Stressed neurons robustly produce *cis* P-tau, *cis* P-tau is released from stressed neurons and neurotoxic, but is effectively blocked by *cis*, but not *trans*, mAb. **a**–**c**, Quantification results of Fig. 4a, b and f, respectively. The results are expressed as means ± s.d. and *P* values determined using the two-way ANOVA test (**a**) and Student's *t*-test (**c**). **d**, Hypoxia induces *cis* P-tau, which is blocked by *cis* mAb. SY5Y neurons expressing a control vector were cultured in the hypoxia chamber in the absence or presence of *cis* or *trans* mAb for the times indicated, followed by immunoblotting for *cis* P-tau. **e**, Hypoxia induces *cis* P-tau before tau aggregation. SY5Y neurons were subjected to hypoxia for the times indicated, followed by sarkosyl extraction before immunoblotting with Tau5 mAb and quantification. **f**, Hypoxia induces cell death, which are blocked by *cis*, but not *trans*, mAb. SY5Y neurons were cultured in the hypoxia chamber in the absence or presence of *cis* or *trans* mAb for the times indicated, followed by live and dead cell assay using the LIVE/DEAD Viability/Cytotoxicity Kit. **g**, Stressed neuron lysates are neurotoxic, which are neutralized by *cis*, but not *trans*, mAb. Cell lysates were prepared from stressed SY5Y neurons and then added to growing SY5Y neurons directly (Control) or after immunodepletion with *cis* or *trans* mAb to remove *cis* or *trans* P-tau, respectively for 3 days, followed by live and dead cell assay. **h**, *Cis* P-tau is released from stressed neurons. SY5Y neurons were cultured in the absence of serum for the times indicated and culture media were collected and centrifuged, followed by analysing the supernatants for *cis* and *trans* P-tau with actin as an indicator of cell lysis.

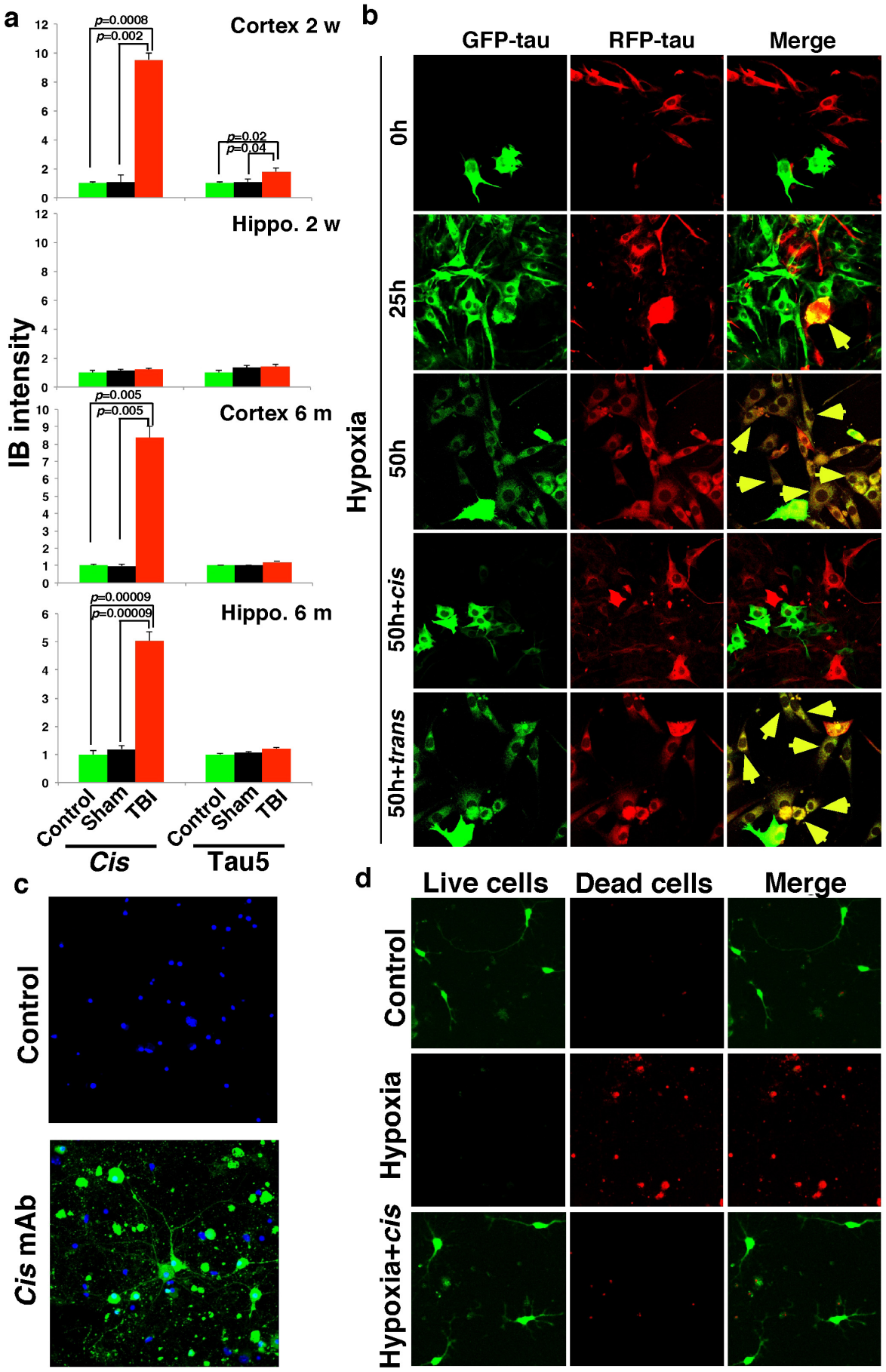

Extended Data Figure 5 | *Cis* P-tau spreads after rmTBI or neuronal stress, and hypoxia induces cell death in primary neurons, which is blocked by *cis* mAb. **a**, *Cis* P-tau spreads in the brain after rmTBI. Quantification results of Fig. 3c. **b**, *Cis* P-tau spreads after neuronal stress. GFP–tau or RFP–tau SY5Y neurons were co-cultured and subjected to hypoxia or control treatment in the presence or absence of *cis* or *trans* mAb for different times, followed by assaying cells expressing both GFP–tau and RFP–tau (arrows) to determine tau spreading among cells. The results are expressed as means ± s.d. and *P* values determined using the Student's *t*-test. **c**, *Cis* mAb enters primary neurons. Primary neurons were established from mouse embryos and differentiated *in vitro* and *cis* mAb was added to culture media, followed by immunostaining with secondary antibodies. **d**, Hypoxia induces cell death in primary neurons, which is effectively blocked by *cis* mAb. Primary neurons were cultured in the hypoxia chamber in the absence or presence of *cis* mAb for 48 h, followed by live (green) and dead (red) cell assay using the LIVE/DEAD Viability/Cytotoxicity Kit.

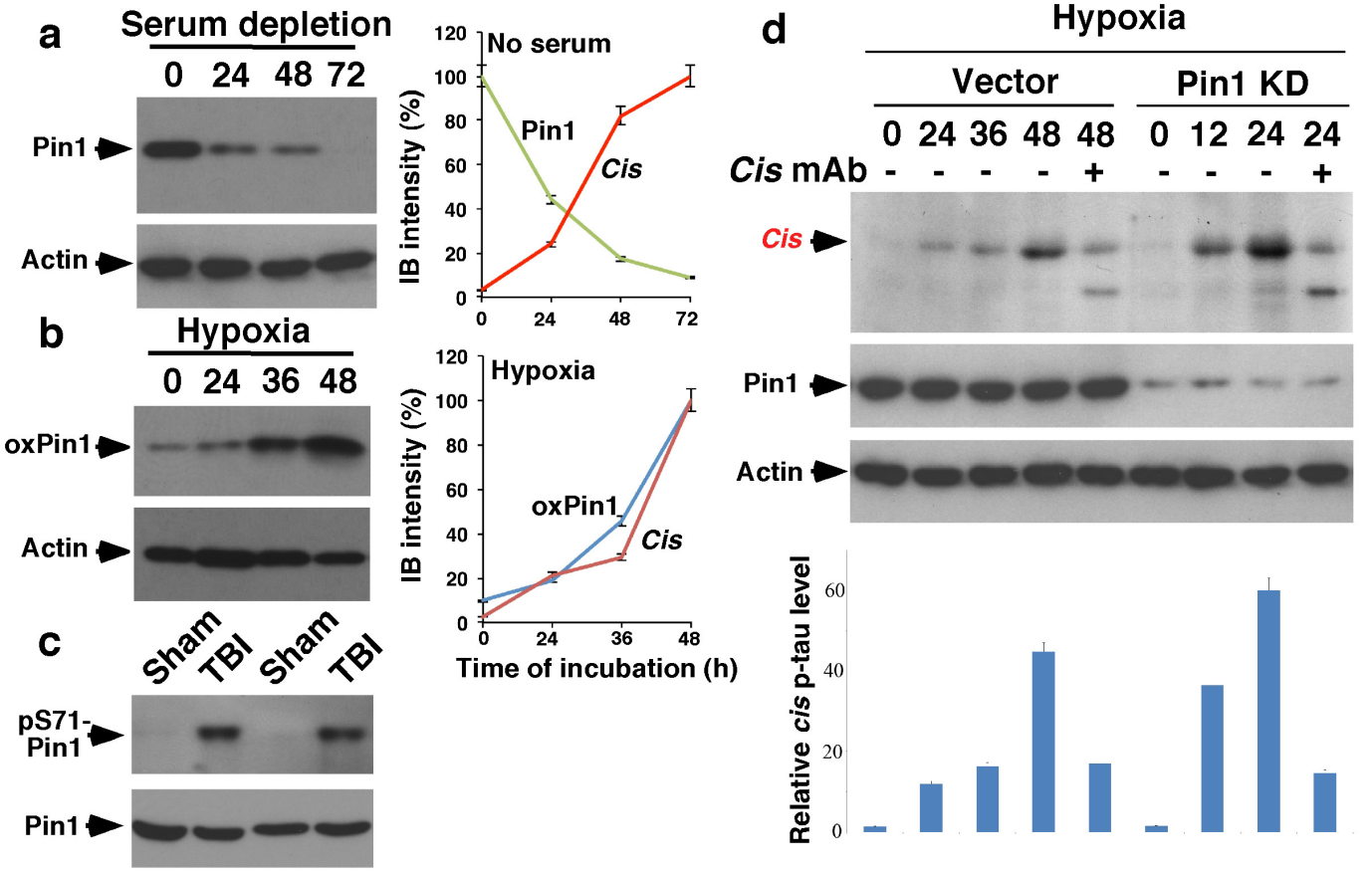

Extended Data Figure 6 | Pin1 inhibition by multiple mechanisms contributes to *cis* P-tau induction after neuron stress and TBI. **a**, Pin1 is downregulated and correlates with *cis* P-tau induction after serum starvation. Cells were subjected to serum starvation for times indicated, followed by immunoblotting, with the right panel showing the correlation of Pin1 down regulation with *cis* P-tau induction from Fig. 4a. **b**, Pin1 is oxidized and correlates with *cis* P-tau induction after hypoxia. SY5Y cells were subjected to hypoxia for times indicated, followed by immunoblotting for C113 oxidized Pin1, with the right panel showing the correlation of Pin1 oxidization with *cis* P-tau induction from Extended Data Fig. 6d. **c**, Pin1 is inhibited in TBI mouse brains. Mouse brains 48 h after ssTBI were subjected to immunoblotting and quantification for Pin1 and S71 phosphorylated Pin1. **d**, Pin1 knockdown potentiates the ability of hypoxia to induce *cis* P-tau. Pin1-knockdown or vector control SY5Y cells were subjected to hypoxia treatment for the times indicated in the presence or absence of *cis* mAb, followed by immunoblotting and quantification for *cis* P-tau levels. The results are expressed as means ± s.d.

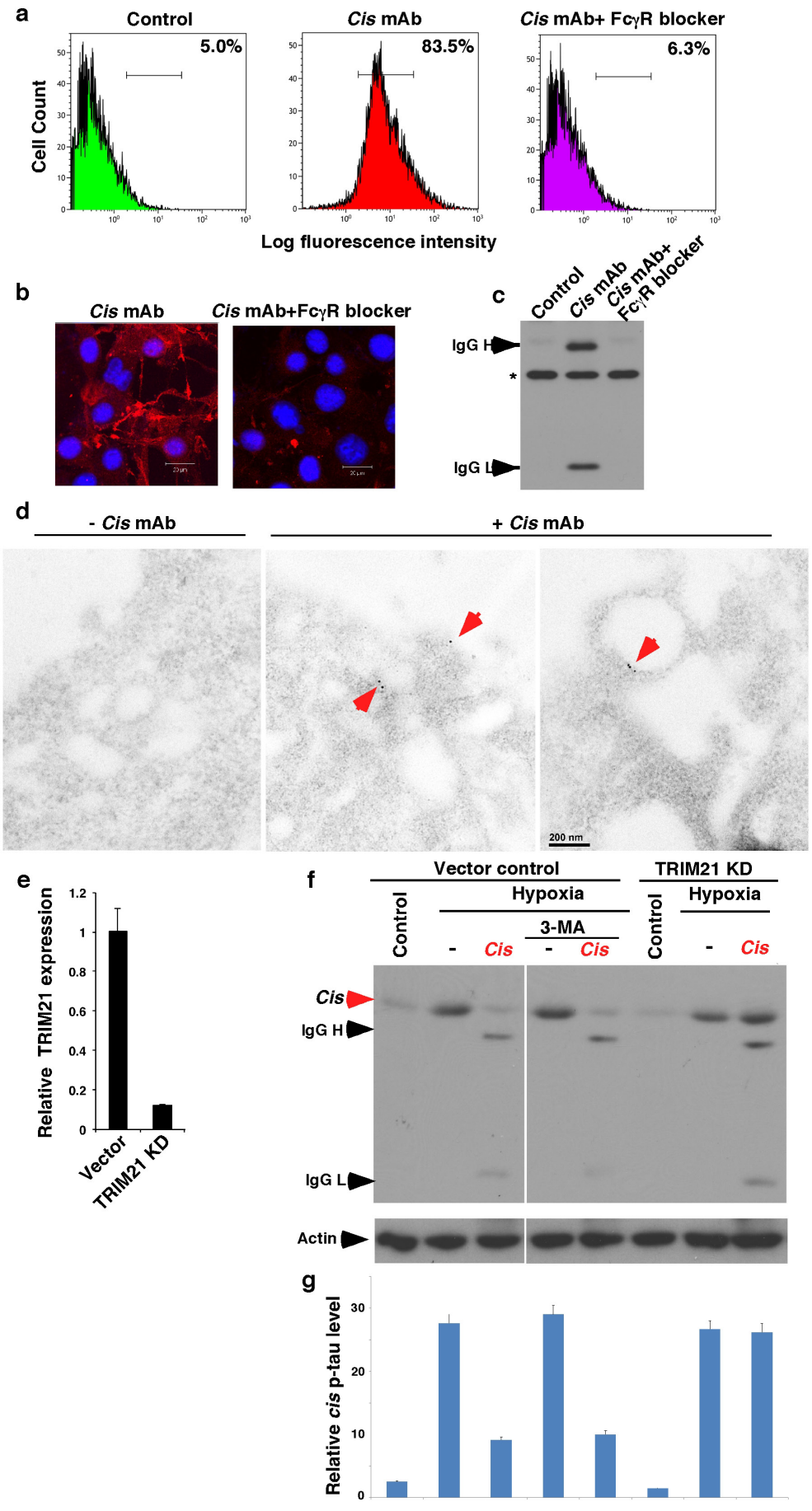

Extended Data Figure 7 | Inhibition of FcγR binding blocks *cis* mAb from entering neurons and TRIM21 KD fully prevented *cis* antibody from ablating *cis* P-tau in neurons. a–d, Inhibition of FcγR binding potently blocks *cis* mAb from entering neurons. *Cis* mAb was added to neurons in the absence or presence of a human FcγR-binding inhibitor, followed by detecting the binding of *cis* mAb to the cell surface by FACS (**a**), entry of *cis* mAb into cells by immunofluorescence (**b**), immunoblotting (**c**) and electron microscopy after immunogold labelling (**d**). The FcR binding inhibitor fully blocked *cis* mAb from binding to the cell surface and entering neurons. Electron microscopy showed that *cis* mAb bound to the cell surface and endocytic vesicles (red arrows). **e**, **f**, TRIM21 knockdown fully prevents *cis* antibody from ablating *cis* P-tau in neurons. TRIM21 was stably knocked down in SY5Y neuronal cells using a validated TRIM21 shRNA lentiviral vector and confirmed by real-time RT–PCR analysis of TRIM21 mRNA expression (**e**). TRIM21 knockdown or vector control SY5Y cells were subjected to hypoxia treatment in the presence or absence of *cis* mAb and/or 3-methyladenine, an autophagy inhibitor, followed by immunoblotting, followed by quantifying *cis* P-tau levels normalized actin levels (lower panel) (**f**). The results are expressed as means ± s.d.

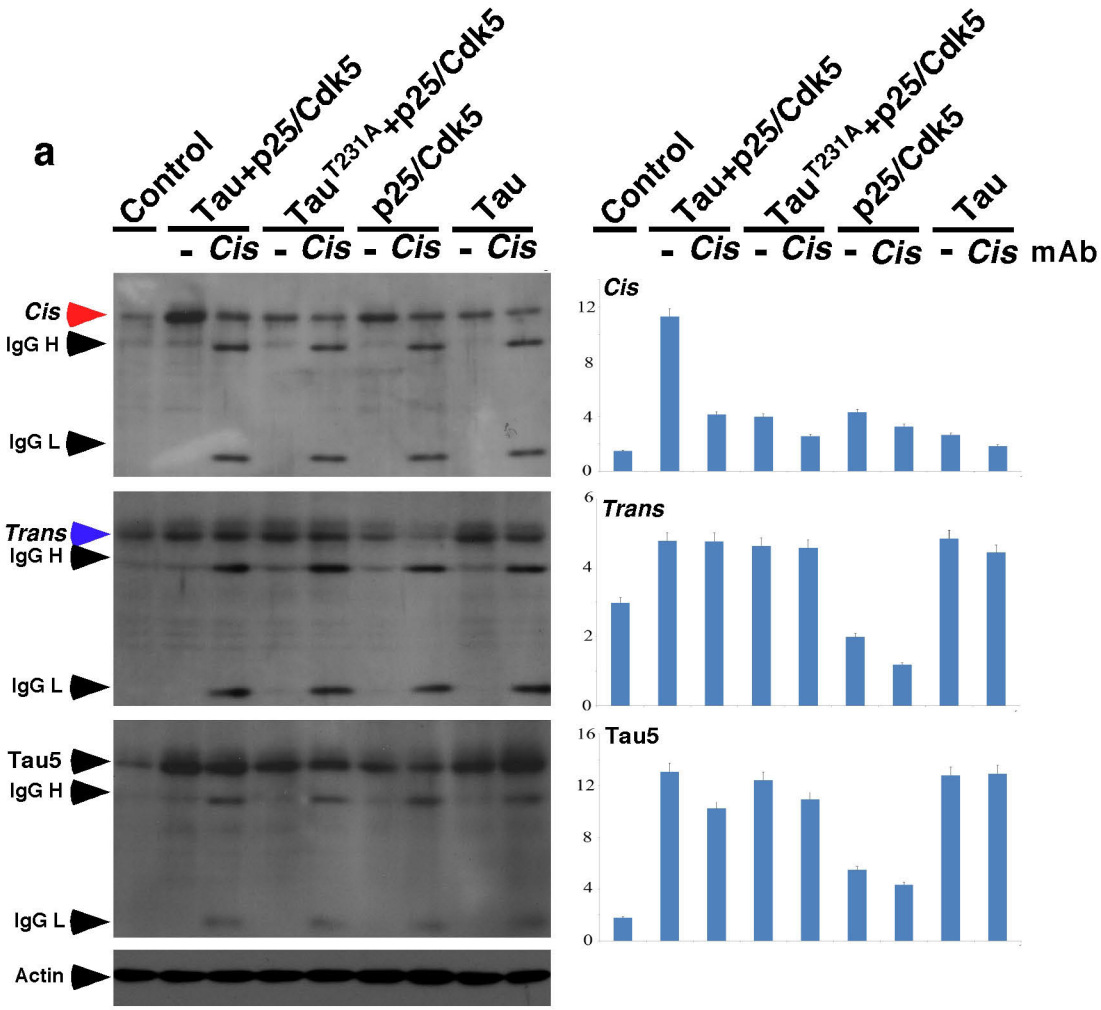

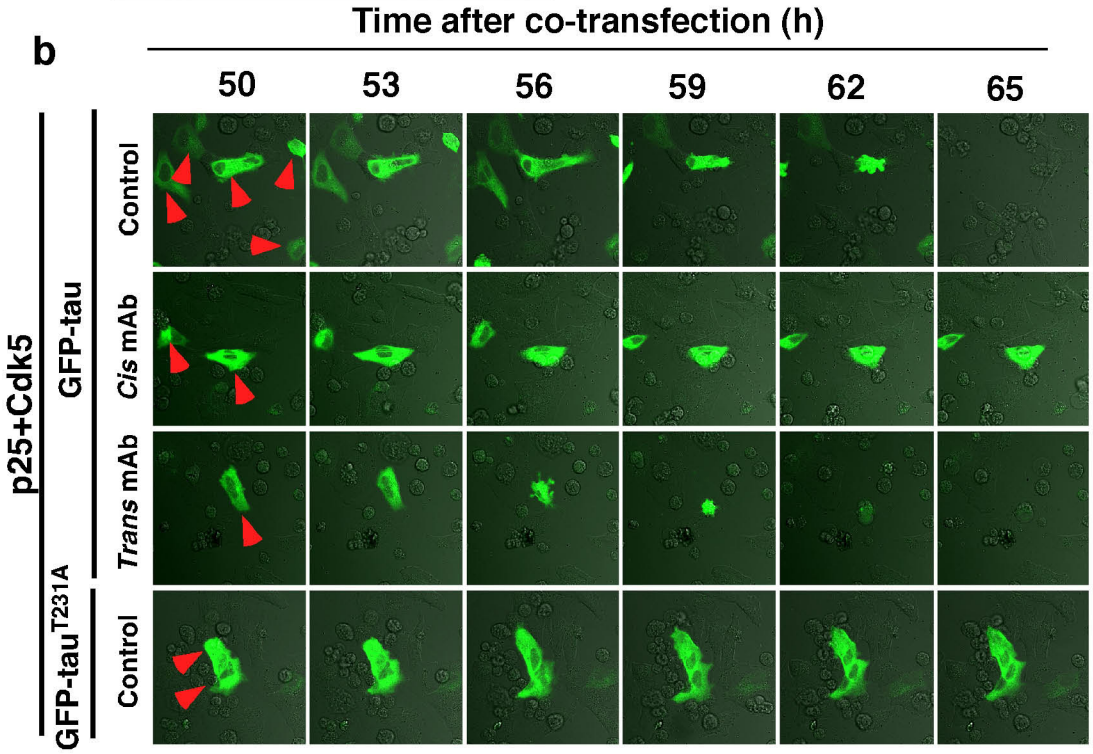

Extended Data Figure 8 | *Cis* pT231-tau is both necessary and sufficient for P-tau to induce neuronal cell death *in vitro*. **a**, SY5Y cells were co-transfected with non-tagged indicated constructs in the absence and presence of *cis* mAb followed by immunoblotting with quantification on the right panel. **b**, SY5Y cells were co-transfected with GFP–tau, or GFP–tau(T231A) and p25/Ckd5 in the absence and presence of *cis* or *trans* mAb followed by live-cell confocal video (see Supplementary Videos 5, 6). Red arrows point to GFP–tau or–tau(T231A) expressing cells. The results are expressed as means ± s.d.

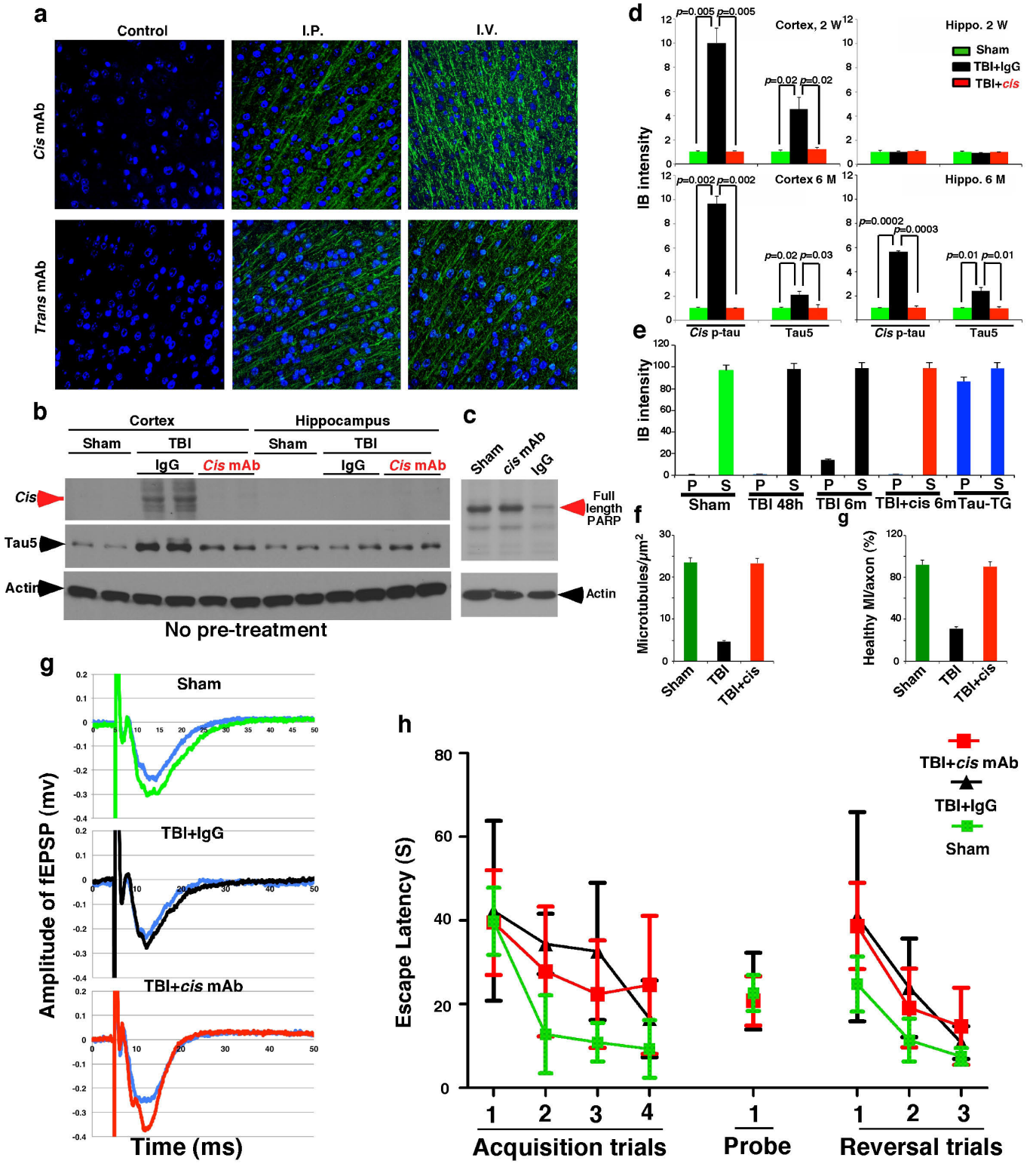

Extended Data Figure 9 | *Cis* mAb effectively blocks *cis* P-tau induction and spread, tau aggregation, and restores neuronal ultrastructures, apoptosis and defective LTP after TBI. **a**, Peripherally administrated *cis* and *trans* mAbs enter neurons in brains. 250 μg of biotinylated *cis* or *trans* mAb was injected intraperitoneally or intravenously into B6 mice, followed by detecting the biotinylated *cis* mAb in brains 3 days later. **b**, **c**, *Cis* mAb effectively blocks *cis* pT231-tau induction and apoptosis. ssTBI mice were randomly and blindly treated with *cis* mAb or IgG isotype control, i.c.v. (intracerebroventricular) 20 μg per mouse 15 min after injury, and then i.p. 200 μg every 4 days for 3 times, followed by subjecting brains to immunoblotting for *cis* P-tau (**b**) and PARP cleavage (**c**), with sham as controls. **d**–**f**, *Cis* mAb effectively blocks *cis* pT231-tau induction and spread, tau aggregation and restores neuronal ultrastructures. ssTBI mice in **c**–**f** received additional i.p. 200 μg per mouse 3 day before injury. **d**, Quantification of immunoblotting in Fig. 5a. **e**, Quantification of immunoblotting in Fig. 5b. **f**, Quantification of electron microscopy images in Fig. 5c. $n = 3$. The results are expressed as means ± s.d. and P values determined using Student's t-test. **g**, *Cis* mAb treatment of ssTBI mice rescues defective LTP in the cortex. fEPSPs were recorded in the layer II/III by stimulating the vertical pathway (the layer V to II/III) in the cortex. Robust LTP was induced by 5 Hz theta-burst in the cortical slices of sham mice ($n = 15$ slices, 9 mice), but was deficient in the cortex of IgG-treated TBI mice ($n = 9$ slices, 5 mice). However, LTP magnitude was restored to the control level in *cis* mAb-treated TBI animals ($n = 9$ slices, 5 mice). The representative recordings were presented. **h**, No significant effects of *cis* pT231-tau mAb treatment on Morris Water Maze performance. 8 weeks after ssTBI, mice underwent Morris Water Maze (MWM) testing consisting of 4 acquisition trials (hidden platform) daily for 4 days (4 runs per trial), a probe trial, followed by a 3 reversal trials (hidden platform) daily for 3 days. Compared to sham mice, injured mice demonstrated increased latency to find the hidden platform in acquisition and reversal trials ($P < 0.001$). There was no difference in injured *cis* mAb mice compared to injured IgG treated mice in acquisition trials ($P = 0.5$) or reversal trial ($P = 0.9$). For probe trials, injured mice performed similarly to sham mice ($P = 0.7$) and injured *cis* mAb treated mice performed similarly to injured IgG treated mice ($P = 0.2$). $n = 4$–7. The results are expressed as means ± s.e.m. and P values determined using ANOVA.

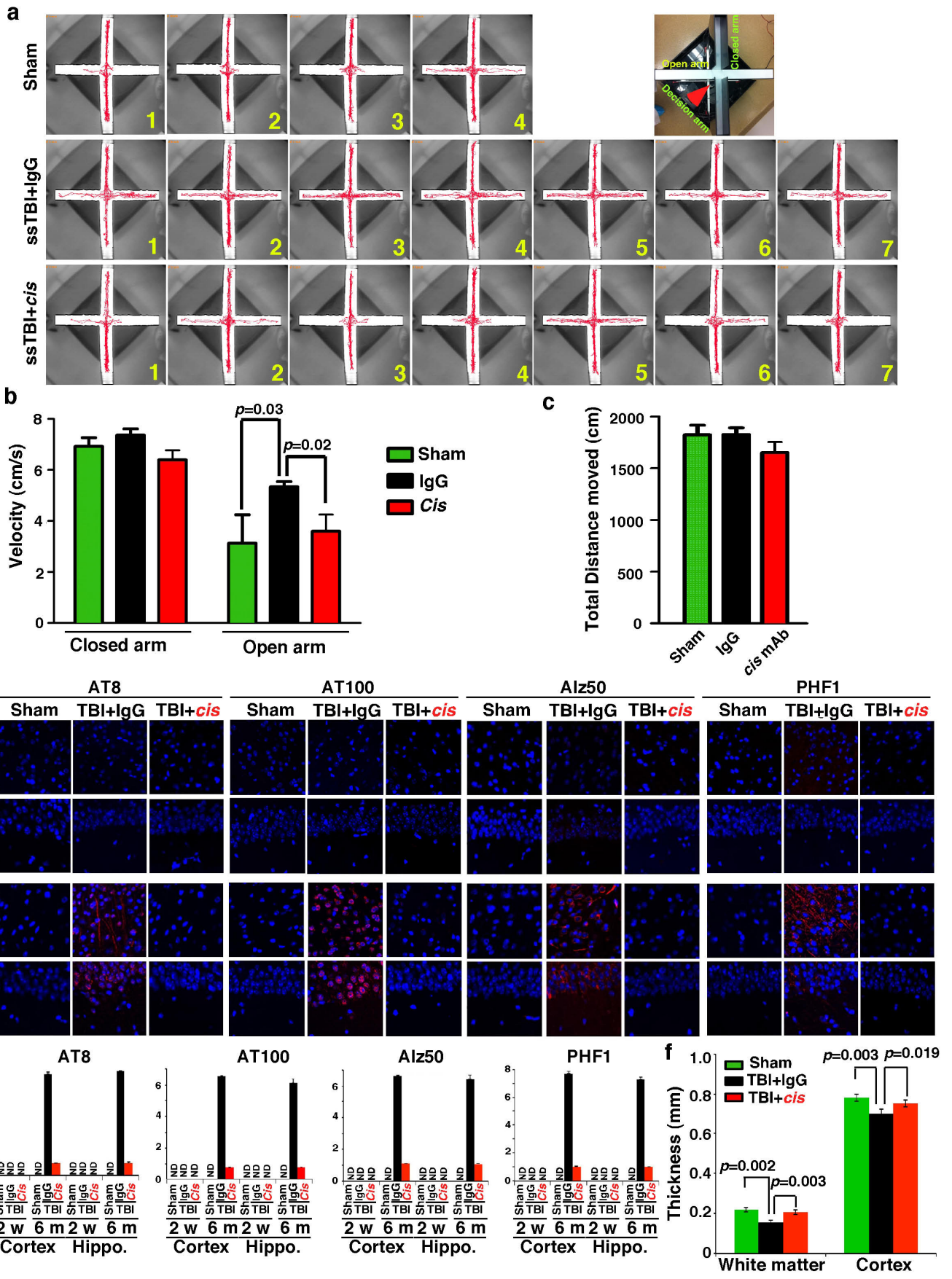

Extended Data Figure 10 | *Cis* mAb treatment effectively restores risk-taking behaviour and prevents tauopathy development and spread as well as brain atrophy after TBI. **a**–**c**, *Cis* mAb treatment effectively restores risk-taking behaviour 2 months after ssTBI. Video-tracking data of each of all mice shows that ssTBI mice treated with *cis* mAb ($n = 7$) spent similar and very little time in the open arm compared to sham mice ($n = 4$), but much less time than TBI mice treated with IgG2b ($n = 7$) (**a**). *Cis* mAb-treated ssTBI mice had similar performance to sham in travelling velocity, but IgG2b-treated ssTBI mice travelled a greater velocity in the open arm (**b**). All three groups travelled similar total distance (**c**). Results are expressed as mean ± S.E.M. and *P* values determined using the Student's *t*-test. **d**–**f**, *Cis* mAb treatment effectively prevents tauopathy development and spread as well as brain atrophy 6 months after ssTBI. ssTBI mice were treated with *cis* mAb or IgG control for 2 weeks or 6 months, with sham mice as controls, followed by immunofluorescence with various tauopathy epitopes (**d**), with immunostaining fluorescence intensity in the cortex and hippocampus being quantified (**e**), or to NeuN immunostaining for determining the thickness of the cortex and white matter at 6 months after TBI (**f**). $n = 4$.